

Gaussian multi-target filtering with target dynamics driven by a stochastic differential equation

Ángel F. García-Fernández, Simo Särkkä *Senior Member, IEEE*

Abstract—This paper proposes multi-target filtering algorithms in which target dynamics are given in continuous time and measurements are obtained at discrete time instants. In particular, targets appear according to a Poisson point process (PPP) in time with a given Gaussian spatial distribution, targets move according to a general time-invariant linear stochastic differential equation, and the life span of each target is modelled with an exponential distribution. For this multi-target dynamic model, we derive the distribution of the set of new born targets and calculate closed-form expressions for the best fitting mean and covariance of each target at its time of birth by minimising the Kullback-Leibler divergence via moment matching. This yields a novel Gaussian continuous-discrete Poisson multi-Bernoulli mixture (PMBM) filter, and its approximations based on Poisson multi-Bernoulli and probability hypothesis density filtering. These continuous-discrete multi-target filters are also extended to target dynamics driven by nonlinear stochastic differential equations.

Index Terms—Poisson multi-Bernoulli mixtures, stochastic differential equations, multi-target filtering.

I. INTRODUCTION

Multi-target filtering consists of estimating the current set of targets given a sequence of past measurements [1]–[3]. It is a fundamental component in many applications including space-object surveillance [4], self-driving vehicles [5] and maritime collision avoidance systems [6]. Target dynamic models usually arise from physics, whose laws are in continuous time, while sensors take measurements at some discrete time steps [7], [8]. In addition, continuous-time dynamic models are decoupled from the sensor sampling times providing a mathematically principled model in scenarios where sensors provide measurements with non-uniform time stamps, for instance, asynchronous multi-rate sensors [9], non-uniform sampling radars [10], [11], event-triggered sensing [12], and the automatic identification system [13]. Therefore, it is important to develop continuous-discrete multi-target filtering algorithms, in which the multi-target dynamics are modelled in continuous time and sensor measurements are provided at some discretised time steps.

Target dynamics in continuous time are usually modelled via stochastic differential equations (SDEs) [8], [14]. Some widely-used dynamic models driven by SDEs are, for example, the Wiener velocity model [8], the Wiener acceleration model [15], the variants of the Ornstein-Uhlenbeck (OU) process

[16]–[18], the coordinated turn model [15], [19] and the re-entry tracking model [20]. In continuous-discrete single-target filtering, we can compute the posterior density of the target by the standard Bayesian filtering recursion, which consists of prediction and update. In this case, the transition density between two time steps can be calculated using the Fokker-Planck-Kolmogorov forward partial differential equation.

With linear and time-invariant SDEs, the transition density is Gaussian and its parameters can be computed via the matrix fraction decomposition [8], [21], [22]. With non-linear SDEs, the transition density is non-Gaussian. In this case, Gaussian assumed density filters can be applied by discretising the SDE first, and then applying a non-linear Gaussian filter prediction step, e.g., an extended or sigma-point Kalman filter [23], [24]. Another alternative is to use assumed density filtering and propagate the mean and covariance matrix through the associated ordinary differential equation (ODE) using analytical linearisation or sigma-points to approximate the required expectations [8], [23]. This approach can be derived from the minimisation of the variational Kullback-Leibler divergence (KLD) [7].

Apart from target dynamics modelled by SDEs, a continuous-time model for multi-target systems must include continuous time models for target appearances and disappearances. As in [25]–[27], we use an M/M/∞ queuing system [28], in which the time of appearance of the targets is a Poisson process, and their life spans are exponentially distributed. The resulting discretised multi-target system is Markovian, with the properties that the target birth model is a Poisson point process (PPP), targets move independently according to the SDE, and targets remain in the scene with a certain probability of survival [25]. If this multi-target system is observed with a standard point-target measurement model, the posterior density of the set of targets is a Poisson multi-Bernoulli mixture (PMBM) [29], [30].

The PMBM filter can be considered a state-of-the-art, fully Bayesian multiple hypothesis tracking algorithm [31], and its multi-target dynamic model considers discrete-time single-target transition densities, a probability of survival at each time step, and a PPP for new born targets at each time step. The PMBM posterior is the union of two independent processes: a PPP that contains information on targets that remain undetected, and a multi-Bernoulli mixture that contains information on potential targets detected at some point up to the current time step. The PPP therefore is very useful in applications where information on occluded objects is important, such as self-driving vehicles and search-and-track applications [32].

A. F. García-Fernández is with ETSI de Telecomunicación, Universidad Politécnica de Madrid, 28040 Madrid, Spain (email: angel.garcia.fernandez@upm.es).

S. Särkkä is with the Department of Electrical Engineering and Automation, Aalto University, 02150 Espoo, Finland (email: simo.sarkka@aalto.fi).

To develop a Gaussian implementation of the continuous-discrete PMBM (CD-PMBM) filter, it is required to approximate the single-target birth density of the PPP for new born targets as a Gaussian and to use the Gaussian prediction step based on the SDE for the single-target densities of surviving targets. Closed-form formulas to obtain an optimal Gaussian fit to the single-target birth density that minimises the KLD for the Wiener velocity model were provided in [25].

While the Wiener velocity model is widely-used in tracking due to its simplicity, it is usually limited to short-term predictions, and is inaccurate in long-term predictions, for instance, due to a possibly unbounded, unrealistic velocity. This limitation can be solved using OU processes, employed in maritime traffic tracking [16], [17], or via more accurate physics-based models such as in space-object tracking [33] and projectile tracking [34]. Therefore, the main goal of this paper is the development of the Gaussian CD-PMBM filters for single-target dynamics driven by linear and non-linear SDEs. The main challenge to develop these multi-target filters is the calculation of the birth process at the discretised time steps. This development enables us to solve multi-target filtering problems with continuous-time dynamics from first mathematical principles.

In this paper, we make these contributions to enable principled multi-target filters with SDE dynamics: 1) Calculation of the closed-form optimal Gaussian approximation of the single-target birth density that minimises the KLD for linear SDEs, without resorting to sampling; 2) Calculation of the single-target birth density when the targets appear with the steady-state solution; 3) Implementation of the Gaussian CD-PMBM filter and related multi-target filters such as the Poisson multi-Bernoulli (PMB) filter [29], the probability hypothesis density (PHD) filter [35] and the cardinality probability hypothesis density (CPHD) filter [35]; 4) The extension of these filters when target dynamics are driven by non-linear SDEs.

The rest of the paper is organised as follows. The problem formulation and background are provided in Section II. The discretised multi-target model is given in Section III. Section IV explains the continuous-discrete Gaussian multi-target filters, and also the extension to non-linear SDEs. Simulation results are analysed in Section V. Finally, conclusions are drawn in Section VI.

II. PROBLEM FORMULATION AND BACKGROUND

In this paper, we are interested in approximating the density of the current set of targets given the sequence of the set of measurements up to the current time step when multi-target dynamics are given in continuous time. The dynamic and measurement models are presented in Section II-A. An overview of the solution in Section II-B. We also provide the required background on integral computations involving matrix exponentials in Section II-C.

A. Multi-target dynamic and measurement models

We consider a multi-target dynamic model in which target appearance, dynamic and disappearance models are in continuous time. The set of targets at a time $t \geq 0$ is denoted

by $X(t) \in \mathcal{F}(\mathbb{R}^{n_x})$, where \mathbb{R}^{n_x} is the single target space, and $\mathcal{F}(\mathbb{R}^{n_x})$ is the space of all finite subsets of \mathbb{R}^{n_x} [35]. Newly appearing targets can be added to $X(t)$ at any t , and disappearing targets can also be removed from $X(t)$ at any time. We consider the continuous-time multi-target model in [25], with the assumptions:

- A1 Target appearance times are distributed according to a Poisson process (in time) with rate $\lambda > 0$ [28].
- A2 At the time a target appears, its distribution is Gaussian with mean \bar{x}_a and covariance matrix P_a , and is independent of the rest of the targets.
- A3 The life span of a target, the time from its appearance to its disappearance, follows an exponential distribution with rate $\mu > 0$ that is independent of any other variable.
- A4 Targets move independently according to a linear time-invariant SDE [8, Eq. (6.1)]

$$dx(t) = Ax(t)dt + udt + Ld\beta(t), \quad (1)$$

where $A \in \mathbb{R}^{n_x \times n_x}$ and $L \in \mathbb{R}^{n_x \times n_\beta}$ are matrices, $dx(t)$ is the differential of $x(t)$, $u \in \mathbb{R}^{n_x}$, and $\beta(t) \in \mathbb{R}^{n_\beta}$ is a Brownian motion with diffusion matrix Q_β .

A sensor obtains measurements from the set of targets $X(t)$ at known time instants t_k , $k \in \mathbb{N}$. The set of targets at time step k , corresponding to time t_k , is $X_k = X(t_k)$ and the set of measurements is $Z_k \in \mathcal{F}(\mathbb{R}^{n_z})$, where \mathbb{R}^{n_z} is the single-measurement space. We consider the standard point-target detection model [35] such that, given X_k , each target $x \in X_k$ is detected with probability $p^D(x)$ generating a measurement with conditional density $l(\cdot|x)$, or missed with probability $1 - p^D(x)$. The set Z_k contains these target-generated measurements and clutter measurements, which are distributed according to a PPP in \mathbb{R}^{n_z} with intensity $\lambda^C(\cdot)$.

B. Overview of the solution

In this paper, we discretise the continuous-time dynamic model in the previous section at the time steps that the measurements are received. This results in a standard multi-target dynamic model with a time-varying probability of survival, single-target transition density and a PPP birth process [25]. Together with the measurement model, this implies that the density $f_{k|k'}(\cdot)$ of X_k given the sequence of measurements $(Z_1, \dots, Z_{k'})$, with $k' \in \{k-1, k\}$, is a PMBM [29], [30].

The PMBM is the union of two independent processes: a PPP with density $f_{k|k'}^P(\cdot)$, representing targets that have not been detected yet, and a multi-Bernoulli mixture (MBM) with density $f_{k|k'}^{\text{mbm}}(\cdot)$, representing targets that have been detected at some point in the past. The PMBM density is

$$f_{k|k'}(X_k) = \sum_{Y \cup W = X_k} f_{k|k'}^P(Y) f_{k|k'}^{\text{mbm}}(W), \quad (2)$$

$$f_{k|k'}^P(X_k) = e^{-\int \lambda_{k|k'}(x) dx} \prod_{x \in X_k} \lambda_{k|k'}(x), \quad (3)$$

$$f_{k|k'}^{\text{mbm}}(X_k) = \sum_{a \in \mathcal{A}_{k|k'}} w_{k|k'}^a \sum_{\substack{\mathfrak{U}_{l=1}^{n_{k|k'}} \\ X^l = X_k}} \prod_{i=1}^{n_{k|k'}} f_{k|k'}^{i,a^i}(X^i), \quad (4)$$

where $\lambda_{k|k'}(\cdot)$ is the PPP intensity, $\mathcal{A}_{k|k'}$ is the set of global hypotheses, $w_{k|k'}$ is the weight of global hypothesis $a = (a^1, \dots, a^{n_{k|k'}}) \in \mathcal{A}_{k|k'}$, $n_{k|k'}$ is the number of Bernoulli components, a^i is the index for the local hypotheses of the i -th Bernoulli component and $f_{k|k'}^{i,a^i}(\cdot)$ is the density of the i -th Bernoulli component with local hypothesis a^i . Index $a^i \in \{1, \dots, h_{k|k'}^i\}$, where $h_{k|k'}^i$ is the number of local hypotheses for the i -th Bernoulli. The symbol \uplus represents the disjoint union and the sum in (2) is taken over all mutually disjoint (and possibly empty) sets Y and W whose union is X_k . A complete explanation of the PMBM density as well as the PMBM filtering recursion for a discrete-time multi-target dynamic model can be found in [29], [30].

In this paper, we will develop the Gaussian implementation of the CD-PMBM filter by discretising the multi-target dynamic model resulting from Assumptions A1-A4. Apart from the CD-PMBM filter, we also develop other approximate filters with lower computational burden. For example, the (track-oriented) PMB filter approximates the posterior as a PMB by performing KLD minimisation after each update using auxiliary variables [29], [36]. The PHD filter and CPHD filters are obtained by approximating the posterior after each update step as a PPP and an independent identically distributed cluster process, respectively, by minimising the KLD [35], [37], [38].

C. Integral computations

To develop the Gaussian implementation of the CD-PMBM filter, we will require to calculate the following types of integrals involving matrix exponentials [22], [39]. The identity matrix of size p is denoted by I_p . When $p = n_x$, we just use the notation I . The zero-matrix of size $m \times n$ is denoted by $0_{m,n}$.

1) *Integral of type 1:* For any $n_x \times n_x$ matrix A and $n_x \times p$ matrix B , we have [22]

$$\begin{aligned} H(t) &= \int_0^t \exp(A\tau) B d\tau \\ &= \begin{bmatrix} I & 0_{n_x,p} \end{bmatrix} \exp(H_c^1 t) \begin{bmatrix} 0_{n_x,p} \\ I_p \end{bmatrix}, \end{aligned} \quad (5)$$

where

$$H_c^1 = \begin{bmatrix} A & B \\ 0_{p,n_x} & 0_{p,p} \end{bmatrix}. \quad (6)$$

Matrix exponentials can be computed using standard mathematical software. In addition, the matrix multiplication on the left and the right of the matrix exponential in (5) just select the top right submatrix of $\exp(H_c^1 t)$ of dimensions $n_x \times p$. Therefore, in the implementation, rather than performing these matrix multiplications, we can just select the corresponding submatrix.

2) *Integral of type 2:* Given the $n_x \times n_x$ matrices A and Q_c , the following equality holds [22]

$$\int_0^t \exp(A\tau) Q_c \exp(A^T \tau) d\tau = F_2^T(t) G_1(t), \quad (7)$$

where

$$\exp(H_c^2 t) = \begin{bmatrix} F_1(t) & G_1(t) \\ 0 & F_2(t) \end{bmatrix}, \quad (8)$$

$$H_c^2 = \begin{bmatrix} -A & Q_c \\ 0 & A^T \end{bmatrix}. \quad (9)$$

3) *Integral of type 3:* Given the $n_x \times n_x$ matrices B , Q_c , and A , the following equality holds

$$\int_0^t \exp(B\tau) Q_c \left[\int_0^\tau \exp(Ar) dr \right] d\tau = \exp(Bt) H_3(t), \quad (10)$$

where

$$\exp(H_c^3 t) = \begin{bmatrix} F_3(t) & G_3(t) & H_3(t) \\ 0 & F_4(t) & G_4(t) \\ 0 & 0 & F_5(t) \end{bmatrix}, \quad (11)$$

and

$$H_c^3 = \begin{bmatrix} -B & Q_c & 0 \\ 0 & 0 & I \\ 0 & 0 & A \end{bmatrix}. \quad (12)$$

Equation (10) is proved in Appendix A.

III. DISCRETISED MULTI-TARGET DYNAMIC MODEL

This section explains the discretisation of the continuous-time multi-target model explained in Section II. In particular, for each time step, we need to calculate the probability of survival (Section III-A), the single-target transition density (Section III-B) and the birth process (Section III-C). The birth process when the mean and covariance at appearance time are given by the steady-state solution of the SDE is provided in Section III-D. We use the notation $\Delta t_k = t_k - t_{k-1}$ to denote the time difference between time steps k and $k-1$.

A. Probability of survival

The probability that a target that was alive at time step t_{k-1} is alive at time step t_k is the probability p_k^S of survival at time step k . Using Assumption A3, its value is [25]

$$p_k^S = e^{-\mu \Delta t_k}. \quad (13)$$

B. Single-target transition density

For an SDE of the form (1), the transition density from time t_{k-1} to t_k is a Gaussian of the form [8, Sec. 6.2]

$$g_k(x(t_k) | x(t_{k-1})) = \mathcal{N}(x(t_k); F_k x(t_{k-1}) + b_k, Q_k), \quad (14)$$

where

$$F_k = \exp(A \Delta t_k), \quad (15)$$

$$b_k = \int_0^{\Delta t_k} \exp(A\tau) d\tau u, \quad (16)$$

$$Q_k = \int_0^{\Delta t_k} \exp(A\tau) L Q_\beta L^T \exp(A\tau)^T d\tau. \quad (17)$$

It should be noted that (16) and (17) can be computed using (5) and (7), respectively.

C. Birth process

From time t_{k-1} to t_k , there are targets that appear and disappear according to A1 and A3. The new born targets at time step k are then the targets that appeared at some time between t_{k-1} and t_k , and remain alive at time t_k . It turns out that, under A1-A4, the distribution of the new born targets is a PPP [25], which we proceed to characterise.

The cardinality distribution $\rho_k^b(\cdot)$ of the new born targets at time step k is [25]

$$\rho_k^b(n) = \mathcal{P}\left(n; \frac{\lambda}{\mu} (1 - e^{-\mu\Delta t_k})\right), \quad (18)$$

where $\mathcal{P}(\cdot; a)$ is a Poisson distribution with parameter a . Equation (18) corresponds to the transient solution of an M/M/ ∞ queueing system, with arrival rate λ and service time parameter μ [40].

If a target appears with a time lag t , that is, it appears at a time $t_k - t > t_{k-1}$, its density at the time of birth t_k is a Gaussian $p_k(x_k | t)$ with mean and covariance [8, Sec. 6.2]

$$\mathbb{E}[x_k | t] = \exp(At) \bar{x}_a + \int_0^t \exp(A\tau) d\tau u, \quad (19)$$

$$\begin{aligned} \mathbb{C}[x_k | t] &= \exp(At) P_a \exp(A^T t) \\ &+ \int_0^t \exp(A\tau) LQ_\beta L^T \exp(A^T \tau) d\tau, \end{aligned} \quad (20)$$

where the integrals are of the form in (5) and (7), and \bar{x}_a and P_a are the mean and covariance matrix at the time of appearance, see A2.

The distribution of the time lag t of new born targets at time step k is a truncated exponential with parameter μ in the interval $[0, \Delta t_k]$, whose density is [25]

$$p_k(t) = \frac{\mu}{1 - e^{-\mu\Delta t_k}} e^{-\mu t} \chi_{[0, \Delta t_k)}(t). \quad (21)$$

Therefore, the single target birth density of the PPP for new born targets is

$$p_k(x_k) = \int_0^{\Delta t_k} p_k(x_k | t) p_k(t) dt. \quad (22)$$

Using (18), the new born target PPP intensity is

$$\lambda_k^B(x_k) = \frac{\lambda}{\mu} (1 - e^{-\mu\Delta t_k}) p_k(x_k). \quad (23)$$

1) *Best Gaussian KLD fit to the birth process:* In this paper, we pursue a Gaussian implementation of the continuous-discrete multi-target filters. To do so, we make a Gaussian approximation to the single target birth density (22) by calculating its mean and covariance matrix. The resulting Gaussian birth PPP is the best fit to the true birth PPP, with intensity (23), from a KLD minimisation perspective [25, Prop. 1]. The mean and covariance matrix of the single-target birth density are provided in the following proposition.

Proposition 1. *Under Assumptions A1-A4, the mean at the time of birth of a single target is*

$$\bar{x}_{b,k} = \mathbb{E}[\mathbb{E}[x_k | t]] \quad (24)$$

$$= \bar{x}_{b,k,1} + \bar{x}_{b,k,2}, \quad (25)$$

where

$$\bar{x}_{b,k,1} = \frac{\mu}{1 - e^{-\mu\Delta t_k}} \begin{bmatrix} I & 0_{n_x,1} \end{bmatrix} \exp(\bar{A}_b \Delta t_k) \begin{bmatrix} 0_{n_x,1} \\ 1 \end{bmatrix},$$

$$\bar{x}_{b,k,2} = \frac{\mu}{1 - e^{-\mu\Delta t_k}} \begin{bmatrix} I & 0_{n_x,2} \end{bmatrix} \exp(\bar{A}_{b,u} t) \begin{bmatrix} 0_{n_x+1,1} \\ 1 \end{bmatrix},$$

and

$$\bar{A}_b = \begin{bmatrix} A - \mu I & \bar{x}_a \\ 0_{1,n_x} & 0 \end{bmatrix}, \quad (26)$$

$$\bar{A}_{b,u} = \begin{bmatrix} A - \mu I & u & 0_{n_x,1} \\ 0_{1,n_x} & -\mu & 1 \\ 0_{1,n_x+1} & 0 & 0 \end{bmatrix}. \quad (27)$$

The covariance matrix at the time of birth of a single target is

$$P_{b,k} = \mathbb{C}[\mathbb{E}[x_k | t]] + \mathbb{E}[\mathbb{C}[x_k | t]], \quad (28)$$

where

$$\begin{aligned} \mathbb{E}[\mathbb{C}[x_k | t]] &= -\frac{1}{1 - e^{-\mu\Delta t_k}} \left[e^{-\mu\Delta t_k} \int_0^{\Delta t_k} \exp(A\tau) \right. \\ &\times LQ_\beta L^T \exp(A^T \tau) d\tau \\ &+ \int_0^{\Delta t_k} \exp((A - \mu/2I)t) C_b \\ &\left. \times \exp((A - \mu/2I)^T t) dt \right], \end{aligned} \quad (29)$$

$$\mathbb{C}[\mathbb{E}[x_k | t]] = \Sigma_{xx} + \Sigma_{xu} + \Sigma_{xu}^T + \Sigma_{uu} - \bar{x}_{b,k} \bar{x}_{b,k}^T, \quad (30)$$

where

$$C_b = LQ_\beta L^T + \mu P_a, \quad (31)$$

and

$$\begin{aligned} \Sigma_{xx} &= \frac{\mu}{1 - e^{-\mu\Delta t_k}} \int_0^{\Delta t_k} \exp((A - \mu/2I)t) \bar{x}_a \bar{x}_a^T \\ &\times \exp((A - \mu/2I)^T t) dt, \end{aligned} \quad (32)$$

$$\begin{aligned} \Sigma_{xu} &= \frac{\mu}{1 - e^{-\mu\Delta t_k}} \int_0^{\Delta t_k} \exp((A - \mu I)t) \bar{x}_a u^T \\ &\times \left(\int_0^t \exp(A^T \tau) d\tau \right) dt, \end{aligned} \quad (33)$$

$$\Sigma_{uu} = -\Sigma_{uu,1} + \Sigma_{uu,2} + \Sigma_{uu,2}^T, \quad (34)$$

$$\begin{aligned} \Sigma_{uu,1} &= \frac{e^{-\mu\Delta t_k}}{1 - e^{-\mu\Delta t_k}} \int_0^{\Delta t_k} \exp(A\tau) d\tau u u^T \\ &\times \int_0^{\Delta t_k} \exp(A^T \tau) d\tau, \end{aligned} \quad (35)$$

$$\begin{aligned} \Sigma_{uu,2} &= \frac{1}{1 - e^{-\mu\Delta t_k}} \int_0^{\Delta t_k} \exp((A - \mu I)t) u u^T \\ &\times \left(\int_0^t \exp(A^T \tau) d\tau \right) dt. \end{aligned} \quad (36)$$

The integrals (29) and (32) can be computed using (7). The integrals in (35) can be computed using (5). The integrals (33) and (36) can be computed using (10).

The proof of Proposition 1 is provided in Appendix B. It should be noted that \bar{A}_b and $\bar{A}_{b,u}$ are square matrices of

order $n_x + 1$ and $n_x + 2$, respectively. The mean $\bar{x}_{b,k}$ and covariance matrix $P_{b,k}$ depend on the disappearance rate μ of the targets, the SDE, and the density of the targets at the time of appearance, characterised by the mean \bar{x}_a and covariance matrix P_a . In addition, the intensity of the PPP also depends on the appearance rate λ of new targets, see (23). Therefore, the Gaussian birth PPP depends on all the parameters of the multi-target dynamic system. It should also be noted that the second term in (29) plus Σ_{xx} can be computed with a single matrix exponential, and the same happens with $\Sigma_{xu} + \Sigma_{uu,2}$.

Example 2. We consider a one dimensional target with state $x = [p, v]^T$, where p is its position and v its velocity. Its mean and covariance matrix at appearing time are $\bar{x}_a = [0, 0]^T$ and $P_a = I_2$, with units in the international system. The target moves with the SDE (1) with

$$A = \begin{bmatrix} 0 & 1 \\ 0 & -\gamma \end{bmatrix}, u = \begin{bmatrix} 0 \\ \gamma \bar{v} \end{bmatrix}, L = \begin{bmatrix} 0 \\ 1 \end{bmatrix}, \quad (37)$$

with $\gamma = 0.2$, $\bar{v} = 10$, $Q_\beta = 1$. The velocity element of this SDE corresponds to a mean-reverting Ornstein-Uhlenbeck (OU) process, similar to the one in [17], with long-run mean velocity \bar{v} . The target life span rate is $\mu = 0.01$.

We draw $2 \cdot 10^5$ samples from the single target birth density (22) first with $\Delta t_k = 1$ s and then with $\Delta t_k = 2$ s. We obtain the best Gaussian fit to the single target birth density, using Proposition 1, and draw $2 \cdot 10^5$ samples from this process. The resulting normalised histograms with $\Delta t_k = 1$ s and $\Delta t_k = 2$ s are shown in Figure 1. We can see that, despite the fact that the mean velocity at the time of appearance is 0, the mean velocity increases at the time of birth, as the SDE process tends to have a mean velocity \bar{v} . The target can move a longer distance and gather more speed in $\Delta t_k = 2$ s than in $\Delta t_k = 1$ s. In addition, for $\Delta t_k = 1$ s, the best Gaussian fit is closer to the true birth density than with $\Delta t_k = 2$ s.

We have also fitted a Gaussian distribution via moment matching using the samples from (22). The resulting KLDs between this Gaussian, and the Gaussian obtained using Proposition 1 for $\Delta t_k = 1$ s and $\Delta t_k = 2$ s are $6.28 \cdot 10^{-6}$ and $7.03 \cdot 10^{-6}$, respectively [41]. As expected, these KLDs are close to zero. Nevertheless, the results of Proposition 1 are obtained at a fraction of the computational cost of the sampled-based approximation. \square

2) *Birth process via state augmentation:* The mean and covariance matrix of the birth process, given by (25) and (28), can also be computed via state augmentation. That is, it is possible to write an equivalent SDE to (1) with an augmented state $s(t)$ that stacks $x(t)$ and the non-zero elements of u . The mean and covariance at the time of birth can then be computed by Proposition 1 using matrix exponentials of higher dimensions, but removing the terms associated with u . This approach can be beneficial for low-dimensional states but becomes less effective as the dimensionality increases, since computing the matrix exponential of a matrix of size n has a computational complexity $O(n^3)$ [42].

To analyse this, Table I shows the mean execution times over 1000 Monte Carlo runs for the calculations of the birth parameters used in Example 2 with variable state dimension.

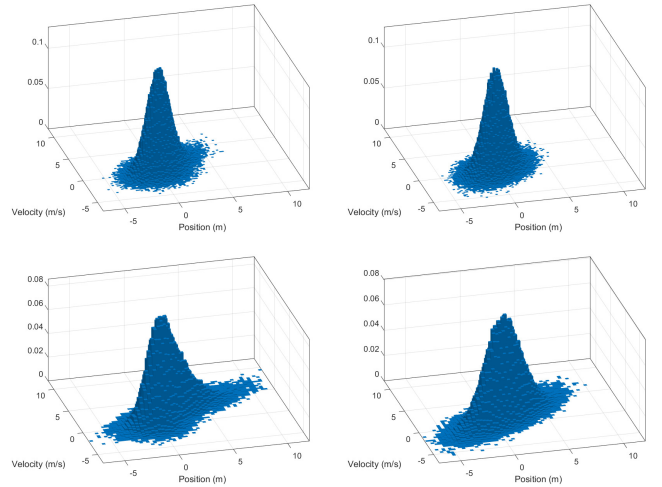


Figure 1: Normalised histograms of Example 2 with samples from the single target birth density (22) with $\Delta t_k = 1$ s (top left), from its best Gaussian fit with $\Delta t_k = 1$ s (top right), from the single target birth density with $\Delta t_k = 2$ s (bottom left), and its best Gaussian fit $\Delta t_k = 2$ s (bottom right).

Table I: Mean execution time (s) to compute the mean and covariance matrix at time of birth

State dimension n_x	Standard state	Augmented state
2	$2.54 \cdot 10^{-4}$	$1.74 \cdot 10^{-4}$
4	$2.65 \cdot 10^{-4}$	$1.89 \cdot 10^{-4}$
10	$4.99 \cdot 10^{-4}$	$5.59 \cdot 10^{-4}$
20	0.0012	0.0018
40	0.0044	0.0100

These times were obtained with a Matlab implementation on an Intel core i5 laptop. We can see that, in this example, the state augmentation approach is faster to compute the birth parameters than the standard approach for state dimensions 2 and 4, but it is slower for state dimensions 10 to 40. Nevertheless, these computational times (for both standard state and augmented state) do not have any impact on the computational burden of the multi-target filters in the simulated scenarios, as there are other parts of a multi-target filter that take longer time, e.g., the data association problem.

D. Steady-state mean and covariance at appearance time

The SDE (1) admits a steady-state solution if the matrix A is Hurwitz, which is a matrix whose eigenvalues have real parts that are strictly negative [8], [43, Sec. 6.5]. In this case, as all the eigenvalues of A are different from zero, A is invertible and the steady-state mean \bar{x}_∞ and covariance P_∞ are

$$\bar{x}_\infty = -A^{-1}u, \quad (38)$$

$$P_\infty = \int_0^\infty \exp(A\tau) L Q_\beta L^T \exp(A^T \tau) d\tau, \quad (39)$$

where (39) is the solution to the Lyapunov equation

$$0 = AP_\infty + P_\infty A^T + LQ_\beta L^T. \quad (40)$$

Then, the following lemma holds.

Lemma 3. *Given a Hurwitz matrix A in the SDE (1), if the mean and covariance at time of appearance are the steady-state ones, $\bar{x}_a = \bar{x}_\infty$ and $P_a = P_\infty$, given by (38) and (39),*

the mean and covariance matrix at the time of birth are the steady-state ones

$$\bar{x}_{b,k} = \bar{x}_\infty, P_{b,k} = P_\infty, \quad (41)$$

$$E[x_k | t] = \bar{x}_\infty, C[x_k | t] = P_\infty. \quad (42)$$

Lemma 3 is proved in Appendix C. This lemma implies that, under the steady-state appearance conditions, it is not required to calculate the integrals in Proposition 1 to calculate the mean $\bar{x}_{b,k}$ and covariance $P_{b,k}$ at the time of birth, as they correspond to the steady-state ones, which can be calculated offline. In addition, it should be noted that, in this case, the birth density is actually Gaussian, while in the general setting, the birth density is approximated as Gaussian, as was illustrated in Example 2. An example of a dynamic model in which A is a Hurwitz matrix is the mixed OU process in [18] in which both the position and velocity components include drift terms.

IV. CONTINUOUS-DISCRETE GAUSSIAN MULTI-TARGET FILTERS

The discretised multi-target dynamic model in the previous section has a linear/Gaussian single-target transition density (14), a state-independent probability of survival (13), and a PPP birth model with intensity (23) that is approximated as Gaussian with mean (25) and covariance matrix (28). For this multi-target dynamic model and the measurement model in Section II-A, we can directly apply the PMBM, PMB, PHD and CPHD filters, see Section II-B, giving rise to their continuous-discrete versions, which we refer to as CD-PMBM, CD-PMB, CD-PHD and CD-CPHD filters. These filters can also be directly implemented if the target appearance model is a Gaussian mixture instead of Gaussian by applying Proposition 1 to each component [25, Sec. IV.D and Lem. 6].

The Gaussian implementations of these filters can then be obtained by considering a constant probability p^D of detection, and a linear and Gaussian single measurement density $l(z|x) = \mathcal{N}(z; Hx, R)$ [29], [30], [44], [45]. The resulting Gaussian CD-PMBM filtering recursion is provided in Section IV-A. In Section IV-B, we also explain how to compute the intensity of the targets that have never been detected in the CD-PMBM filter when the targets appear with the steady-state mean and covariance matrix. We also show how to extend these filters when the SDE is non-linear in Section IV-C.

A. Gaussian CD-PMBM filter

In a Gaussian CD-PMBM filter implementation, the PPP intensity is an unnormalised Gaussian mixture

$$\lambda_{k|k'}(x) = \sum_{j=1}^{n_{k|k'}^p} w_{k|k'}^{p,j} \mathcal{N}\left(x; \bar{x}_{k|k'}^{p,j}, P_{k|k'}^{p,j}\right), \quad (43)$$

where $n_{k|k'}^p$ is the number of Gaussian components, and $w_{k|k'}^{p,j}$, $\bar{x}_{k|k'}^{p,j}$ and $P_{k|k'}^{p,j}$ are the weight, mean and covariance matrix of the j -th component. The expected number of targets that exist at time step k but have not been detected yet is the sum of the weights $\sum_{j=1}^{n_{k|k'}^p} w_{k|k'}^{p,j}$.

In addition, the single-target density of the i -th Bernoulli with local hypothesis a^i is

$$p_{k|k'}^{i,a^i}(x) = \mathcal{N}\left(x; \bar{x}_{k|k'}^{i,a^i}, P_{k|k'}^{i,a^i}\right), \quad (44)$$

where $\bar{x}_{k|k'}^{i,a^i}$ is the mean and $P_{k|k'}^{i,a^i}$ is the covariance matrix.

The CD-PMBM filter is initiated at time $t = 0$ ($k = 0$), with parameters $\lambda_{0|0}(x) = 0$, $n_{0|0}^p = 0$, $n_{0|0} = 0$. The set $\mathcal{A}_{k|k'}$ of global hypotheses and the local data-association hypotheses are constructed as in the PMBM filter as follows [29]. Let $Z_k = \{z_k^1, \dots, z_k^{m_k}\}$ and (k, j) be a pair to refer to z_k^j . The set of all these pairs up to time step k is \mathcal{M}_k . The local hypothesis a^i for the i -th Bernoulli considers the associations with the measurements pairs in $\mathcal{M}_k^{i,a^i} \subseteq \mathcal{M}_k$, such that in \mathcal{M}_k^{i,a^i} there can be at maximum one measurement per time step. The set $\mathcal{A}_{k|k'}$ then contains all possible $(a^1, \dots, a^{n_{k|k'}})$ such that $\bigcup_{i=1}^{n_{k|k'}} \mathcal{M}_k^{i,a^i} = \mathcal{M}_k$ and $\mathcal{M}_k^{i,a^i} \cap \mathcal{M}_k^{j,a^j} = \emptyset \forall i \neq j$.

The prediction step for the Gaussian CD-PMBM filter is provided in the following lemma.

Lemma 4 (Prediction). *Let the filtering density at time step $k-1$ (time t_{k-1}) be a PMBM $f_{k-1|k-1}(\cdot)$ of the form (2), with PPP intensity (43) and single-target densities (44). At time step k (time t_k), the predicted CD-PMBM filter parameters are*

$$\begin{aligned} \lambda_{k|k-1}(x) &= p_{S,k} \sum_{j=1}^{n_{k-1|k-1}^p} w_{k-1|k-1}^{p,j} \mathcal{N}\left(x; \bar{x}_{k|k-1}^{p,j}, P_{k|k-1}^{p,j}\right) \\ &+ \frac{\lambda}{\mu} \left(1 - e^{-\mu \Delta t_k}\right) \mathcal{N}\left(x; \bar{x}_{b,k}, P_{b,k}\right), \end{aligned} \quad (45)$$

where $p_{S,k}$ is given by (13), $\bar{x}_{b,k}$ and $P_{b,k}$ are given by Proposition 1, and

$$\bar{x}_{k|k-1}^{p,j} = F_k \bar{x}_{k-1|k-1}^{p,j} + b_k, \quad (46)$$

$$P_{k|k-1}^{p,j} = F_k P_{k-1|k-1}^{p,j} F_k^T + Q_k, \quad (47)$$

where F_k , b_k and Q_k are given in (15), (16) and (17). The predicted parameters of the Bernoulli components $i \in \{1, \dots, n_{k-1|k-1}\}$ are

$$r_{k|k-1}^{i,a^i} = p_{S,k} r_{k-1|k-1}^{i,a^i}, \quad (48)$$

$$\bar{x}_{k|k-1}^{i,a^i} = F_k \bar{x}_{k-1|k-1}^{i,a^i}, \quad (49)$$

$$P_{k|k-1}^{i,a^i} = F_k P_{k-1|k-1}^{i,a^i} F_k^T + Q_k, \quad (50)$$

and $n_{k|k-1} = n_{k-1|k-1}$, $h_{k|k-1}^i = h_{k-1|k-1}^i$, $w_{k|k-1}^{i,a^i} = w_{k-1|k-1}^{i,a^i}$.

The Gaussian CD-PMBM update is the same as in [25] and is given in the following lemma.

Lemma 5 (Update). *Let the predicted density at time step k (time t_k) be a PMBM $f_{k|k-1}(\cdot)$ of the form (2), PPP intensity (43) and single target densities in (44). The updated PMBM at time step k with measurement set $Z_k = \{z_k^1, \dots, z_k^{m_k}\}$ is a PMBM of the form (2) with PPP intensity $\lambda_{k|k}(x) = (1 - p_D) \lambda_{k|k-1}(x)$ and $n_{k|k} = n_{k|k-1} + m_k$ Bernoulli components.*

For each single target hypothesis of the Bernoulli components at previous time steps $i \in \{1, \dots, n_{k|k-1}\}$, the update creates $(m_k + 1)$ single target hypotheses representing a missed detection and an update with one of the measurements, such that $h_{k|k}^i = h_{k|k-1}^i (m_k + 1)$. The parameters for missed detection hypotheses, $i \in \{1, \dots, n_{k|k-1}\}$ $a^i \in \{1, \dots, h_{k|k-1}^i\}$, are $\mathcal{M}_k^{i,a^i} = \mathcal{M}_{k-1}^{i,a^i}$, $\bar{x}_{k|k}^{i,a^i} = \bar{x}_{k|k-1}^{i,a^i}$, $P_{k|k}^{i,a^i} = P_{k|k-1}^{i,a^i}$.

$$w_{k|k}^{i,a^i} = w_{k|k-1}^{i,a^i} \left(1 - r_{k|k-1}^{i,a^i} + r_{k|k-1}^{i,a^i} (1 - p_D) \right), \quad (51)$$

$$r_{k|k}^{i,a^i} = \frac{r_{k|k-1}^{i,a^i} (1 - p_D)}{1 - r_{k|k-1}^{i,a^i} + r_{k|k-1}^{i,a^i} (1 - p_D)}. \quad (52)$$

For a previous Bernoulli component $i \in \{1, \dots, n_{k|k-1}\}$ and previous single target hypothesis $\tilde{a}^i \in \{1, \dots, h_{k|k-1}^i\}$, the new hypothesis generated by measurement z_k^j has $a^i = \tilde{a}^i + h_{k|k-1}^i j$, $r_{k|k}^{i,a^i} = 1$, and $\mathcal{M}_k^{i,a^i} = \mathcal{M}_{k-1}^{i,\tilde{a}^i} \cup \{(k, j)\}$

$$w_{k|k}^{i,a^i} = w_{k|k-1}^{i,\tilde{a}^i} r_{k|k-1}^{i,\tilde{a}^i} p_D \mathcal{N} \left(z_k^j; H \bar{x}_{k|k-1}^{i,\tilde{a}^i}, S_{k|k-1}^{i,\tilde{a}^i} \right), \quad (53)$$

$$\bar{x}_{k|k}^{i,a^i} = \bar{x}_{k|k-1}^{i,\tilde{a}^i} + K_{k|k-1}^{i,\tilde{a}^i} \left(z_k^j - H \bar{x}_{k|k-1}^{i,\tilde{a}^i} \right), \quad (54)$$

$$P_{k|k}^{i,a^i} = P_{k|k-1}^{i,\tilde{a}^i} - K_{k|k-1}^{i,\tilde{a}^i} H P_{k|k-1}^{i,\tilde{a}^i}, \quad (55)$$

$$K_{k|k-1}^{i,\tilde{a}^i} = P_{k|k-1}^{i,\tilde{a}^i} H^T \left(S_{k|k-1}^{i,\tilde{a}^i} \right)^{-1}, \quad (56)$$

$$S_{k|k-1}^{i,\tilde{a}^i} = H P_{k|k-1}^{i,\tilde{a}^i} H^T + R. \quad (57)$$

For the new Bernoulli component created by z_k^j , whose index is $i = n_{k|k-1} + j$, there are two local hypotheses ($h_{k|k}^i = 2$). The first corresponds to a non-existent Bernoulli such that $\mathcal{M}_k^{i,1} = \emptyset$, $w_{k|k}^{i,1} = 1$ and $r_{k|k}^{i,1} = 0$. The second represents that the measurement z_k^j may be clutter or the first detection of a new target, with parameters $\mathcal{M}_k^{i,2} = \{(k, j)\}$

$$w_{k|k}^{i,2} = \lambda^C \left(z_k^j \right) + e \left(z_k^j \right), \quad (58)$$

$$e \left(z_k^j \right) = p_D \sum_{j=1}^{n_{k|k-1}^p} w_{k|k-1}^{p,j} \mathcal{N} \left(z_k^j; H \bar{x}_{k|k-1}^{p,j}, S_{k|k-1}^{p,j} \right), \quad (59)$$

$$r_{k|k}^{i,2} = \frac{e \left(z_k^j \right)}{\lambda^C \left(z_k^j \right) + e \left(z_k^j \right)}, \quad (60)$$

$$\bar{x}_{k|k}^{i,2} = \sum_{l=1}^{n_{k|k-1}^p} w_l^j \bar{x}_l^j, \quad (61)$$

$$P_{k|k}^{i,2} = \sum_{l=1}^{n_{k|k-1}^p} w_l^j \left[P_l + \left(\bar{x}_l^j - \bar{x}_{k|k}^{i,2} \right) \left(\bar{x}_l^j - \bar{x}_{k|k}^{i,2} \right)^T \right], \quad (62)$$

$$w_l^j \propto w_{k|k-1}^{p,l} \mathcal{N} \left(z_k^j; H \bar{x}_{k|k-1}^{p,l}, S_{k|k-1}^{p,l} \right), \quad (63)$$

$$\bar{x}_l^j = \bar{x}_{k|k-1}^{p,l} + K_l \left(z_k^j - H \bar{x}_{k|k-1}^{p,l} \right), \quad (64)$$

$$P_l = P_{k|k-1}^{p,l} - K_l H P_{k|k-1}^{p,l}, \quad (65)$$

$$K_l = P_{k|k-1}^{p,l} H^T \left(S_{k|k-1}^{p,l} \right)^{-1}, \quad (66)$$

$$S_{k|k-1}^{p,l} = H P_{k|k-1}^{p,l} H^T + R. \quad (67)$$

In the Gaussian CD-PMBM implementation, the single-target birth density of the new Bernoulli components is a Gaussian mixture so its mean and covariance, given by (61) and (62), are obtained by moment matching [25]. In addition, in a practical implementation, it is required to prune the number of global hypothesis [46, Sec. V.D]. This can be achieved using standard PMBM pruning techniques: gating, Murty's algorithm, discarding PPP components with low weight, and discarding Bernoulli densities with low probability of existence [30].

B. Undetected target intensity for steady-state appearance model

In this section, we calculate the intensity of the targets that have not been detected yet for the CD-PMBM filter when targets appear with the steady-mean and covariance matrix at appearance time, see Section III-D, and the measurement model has a constant probability p^D of detection.

Lemma 6. *If matrix A in the SDE (1) is Hurwitz, the mean and covariance at time of appearance are the steady-state ones, $\bar{x}_a = \bar{x}_\infty$ and $P_a = P_\infty$, given by (38) and (39), and the probability of detection is a constant p^D , then, the intensity of the targets that remain undetected in the CD-PMBM filter, see (2), is*

$$\lambda_{k|k'}(x) = \bar{\lambda}_{k|k'} \mathcal{N}(x; \bar{x}_\infty, P_\infty), \quad (68)$$

where $\bar{\lambda}_{k|k'}$ can be calculated recursively as follows

$$\bar{\lambda}_{k|k-1} = p_k^S \bar{\lambda}_{k-1|k-1} + \frac{\lambda}{\mu} \left(1 - e^{-\mu \Delta t_k} \right), \quad (69)$$

$$\bar{\lambda}_{k|k} = (1 - p^D) \bar{\lambda}_{k|k-1}, \quad (70)$$

where $\bar{\lambda}_{0|0}$ is the (known) expected number of targets at time step 0 (usually $\bar{\lambda}_{0|0} = 0$) and the probability of survival is $p_k^S = e^{-\mu \Delta t_k}$, see (13).

The proof of (68)-(70) can be directly obtained by applying the PMBM prediction and update for targets that remain undetected [29], and the facts that the birth intensity is (23), and the steady-state mean and covariance do not change in prediction. Therefore, in this case, the prediction and update of the PPP of the PMBM filter just requires the calculation of $\bar{\lambda}_{k|k'}$ using (69) and (70), as \bar{x}_∞ and P_∞ are calculated beforehand. In addition, we can also establish the following lemma for steady-state solutions for $\bar{\lambda}_{k|k-1}$ and $\bar{\lambda}_{k|k}$.

Lemma 7. *If the sampling time interval is a constant Δt and the probability of detection is a constant p^D , then, the probability of survival is a constant p^S given by (13), and the predicted and updated expected number of undetected targets ($\bar{\lambda}_{k|k-1}$ and $\bar{\lambda}_{k|k}$) reach steady-state solutions, given by*

$$\bar{\lambda}_{k|k-1}^\infty = \frac{\bar{\lambda}^B}{1 - p^S + p^S p^D}, \quad (71)$$

$$\bar{\lambda}_{k|k}^\infty = \frac{(1 - p^D) \bar{\lambda}^B}{1 - p^S + p^S p^D}, \quad (72)$$

where the (constant) expected number of new born targets at each time step is $\bar{\lambda}^B = \frac{\lambda}{\mu} (1 - e^{-\mu\Delta t})$,

The proof of Lemma 7 is provided in Appendix D. If the conditions of Lemmas 6 and 7 hold, and the expected number of targets at time step 0 (before any measurements are taken) is $\bar{\lambda}_{0|0} = \bar{\lambda}_{k|k}^\infty$, then the expected number of undetected targets is always $\bar{\lambda}_{k|k-1}^\infty$ in prediction and $\bar{\lambda}_{k|k}^\infty$ in the update, with an intensity of the form (68). This result also indicates when and how the CD-PMBM filter does not need to propagate explicit information on undetected targets to perform tracking on detected targets using first Bayesian principles.

It should be noted that a target dynamic model that admits a steady-state solution is the mixed OU process in [18], [27]. This process can be used to model targets that are likely to move in a certain area, e.g., patrol agents. In this case, choosing a target appearance model that matches the steady-state solution simplifies the CD-PMBM filtering recursion since the PPP intensity is given by Lemma 6, and Lemma 7 for a constant time interval.

C. Extension to nonlinear SDEs

In this section, we extend the results in Sections III and IV to the case in which the targets move with a non-linear time-invariant SDE. We consider Assumptions A1-A3 and

- A5 Targets move independently according to a non-linear time-invariant SDE

$$dx(t) = f(x) dt + L(x) d\beta(t), \quad (73)$$

where $f(x)$ is the drift function and $L(x)$ the dispersion matrix.

In this case, the update step of the Gaussian CD-PMBM is also given by Lemma 5, as A5 only affects the dynamic model. In the prediction step, the probability of survival is also given by (13), and has the form of Lemma 4. Under A5, the difference with the previous results is that the single-target transition density changes. In turn, this implies that the predicted mean and covariance for surviving targets are now calculated as in Section IV-C1, and the mean and covariance of a target at the time of birth are calculated as in Section IV-C2. These results are applied in the same manner to the CD-PMB, CD-PHD and CD-CPHD filters.

1) *Prediction of the mean and covariance matrix:* There are several ways to propagate a mean and a covariance matrix of a target that moves according to the SDE (73) [8, Chap. 9]. Let $m(t)$ and $P(t)$ denote the mean and covariance of a target that moves according to the SDE (73). We use a standard approach based on analytical linearisation of the SDE. In the following, we drop the dependence on t of $m(t)$ and $P(t)$ following the standard notation in SDEs [8].

We linearise the drift function $f(\cdot)$ around the mean m as

$$f(x) \approx f(m) + F_x(m)(x - m), \quad (74)$$

where $F_x(m)$ is the Jacobian of $f(x)$ w.r.t. x , and also approximate the dispersion matrix as

$$L(x) \approx L(m). \quad (75)$$

Under approximations (74) and (75), the mean and covariance of the target at a given time are obtained by solving [8]

$$\frac{dm}{dt} = f(m), \quad (76)$$

$$\frac{dP}{dt} = PF_x^T(m) + F_x(m)P + L(m)QL^T(m). \quad (77)$$

Then, let us consider that the posterior single-target density $p_{k-1|k-1}^{i,a^i}(\cdot)$ is given by (44). Then, we set the initial conditions of the ODE (76)-(77) as $m(0) = \bar{x}_{k-1|k-1}^{i,a^i}$ and $P(0) = P_{k-1|k-1}^{i,a^i}$, and use an ODE solver to set the predicted mean and covariance as $\bar{x}_{k|k-1}^{i,a^i} = m(\Delta t_k)$ and $P_{k|k-1}^{i,a^i} = P(\Delta t_k)$. This operation is also performed for each Gaussian component in the PPP (43).

2) *Mean and covariance at the time of birth:* Let us consider a target that appears with a time lag t . Then, its conditional mean and covariance at the time of birth are

$$E[x_k|t] = m(t), \quad C[x_k|t] = P(t), \quad (78)$$

where $m(t)$ and $P(t)$ are the solution of the ODE (76)-(77) integrated from time 0 to t with initial condition $m(0) = \bar{x}_a$ and $P(0) = P_a$. Note that the analogous equations for a linear SDE are given by (19) and (20). The mean and covariance at the time of birth are then given by the following proposition.

Proposition 8. *Under approximations (74) and (75) and Assumptions A1-A3 and A5, the mean $\bar{x}_{b,k}$ and covariance $P_{b,k}$ of a target at the time of birth are*

$$\bar{x}_{b,k} = \frac{\mu}{1 - e^{-\mu\Delta t_k}} \bar{x}(\Delta t_k), \quad (79)$$

$$P_{b,k} = \frac{\mu}{1 - e^{-\mu\Delta t_k}} \Sigma(\Delta t_k) - \bar{x}_{b,k} \bar{x}_{b,k}^T, \quad (80)$$

where $\bar{x}(\Delta t_k)$ and $\Sigma(\Delta t_k)$ are calculated by solving the ODE

$$\frac{dm}{dt} = f(m), \quad (81)$$

$$\frac{dP}{dt} = PF_x^T(m) + F_x(m)P + L(m)QL^T(m), \quad (82)$$

$$\frac{d\bar{x}}{dt} = m e^{-\mu t}, \quad (83)$$

$$\frac{d\Sigma}{dt} = [P + mm^T] e^{-\mu t}, \quad (84)$$

from $t = 0$ to Δt_k with initial condition $m(0) = \bar{x}_a$, $P(0) = P_a$, $\bar{x}(0) = 0$ and $\Sigma(0) = 0$.

The proof of Proposition 8 is provided in Appendix E. In practice, these ODEs that involve mean and covariances can be solved by stacking the mean and covariances into a single vector and applying an available ODE solver [8].

It should be noted that it is also possible to linearise the drift function and the dispersion matrix as in (74) and (75) at the initial mean \bar{x}_a , and leave the linearisation fixed for the whole interval. With the resulting linearised SDE, the mean and covariance matrix at the time of birth can be computed via Proposition 1. Nevertheless, since the linearisation errors accumulate over time as the mean deviates from its initial value, the provided solution is less accurate than the one provided by Proposition 8, especially for longer time intervals.

V. SIMULATION RESULTS

This section includes the numerical evaluation of the CD-PMBM, CD-PMB, CD-PHD and CD-CPHD filters in a linear and a non-linear SDE scenario¹. In the non-linear scenario, the ODEs are solved using Matlab ode45 solver. The CD-PMBM filter has been implemented with the following parameters: maximum number of global hypotheses $N_h = 200$, threshold for pruning PPP Gaussian components $\Gamma_p = 10^{-5}$, threshold for pruning multi-Bernoulli mixture weights $\Gamma_{mbm} = 10^{-4}$, and threshold for the probability of existence to prune Bernoulli densities $\Gamma_b = 10^{-5}$. The filter also uses ellipsoidal gating with threshold 20 and Estimator 1 in [30], with threshold 0.4. The CD-PMB filter is implemented as the CD-PMBM but projecting the output of the update step to a PMB density [29]. The CD-PHD and CD-CPHD filters have been implemented with a maximum number of components of 30, pruning threshold 10^{-5} and merging threshold 0.1.

We also compare these continuous-discrete filters with the equivalent (discrete-time) PMBM, PMB, PHD and CPHD filters with a fixed sampling time, which is taken to be the minimum Δt_k in the considered time window. These filters can compute offline the birth model parameters, which remain fixed for all time steps, using Proposition 1 or 8. Then, in the linear case, the equivalent linear and Gaussian dynamic model can also be computed offline. In the non-linear case, the propagation of the mean and covariance matrix of the targets can be done following Section IV-C1. These filters only perform the update step at the time steps when measurements have been received. The rest of the parameters of the PMBM, PMB, PHD and CPHD filters are set as indicated above for the continuous-discrete versions.

A. Linear SDE

We consider an OU process for the velocity as in [17]. The state is $x(t) = [p_x(t), v_x(t), p_y(t), v_y(t)]^T$, which contains position and velocity in the x and y coordinates. The SDE parameters are

$$A = \begin{bmatrix} 0 & 1 & 0 & 0 \\ 0 & -\gamma & 0 & 0 \\ 0 & 0 & 0 & 1 \\ 0 & 0 & 0 & -\gamma \end{bmatrix}, u = \begin{bmatrix} 0 \\ \gamma \bar{v}_x \\ 0 \\ \gamma \bar{v}_y \end{bmatrix}, L = \begin{bmatrix} 0 & 0 \\ 1 & 0 \\ 0 & 0 \\ 0 & 1 \end{bmatrix},$$

and $Q_\beta = qI_2$. The numerical values of these parameters are $\gamma = 0.1 \text{ (s}^{-1}\text{)}$, $\bar{v}_x = 1 \text{ (m/s)}$, $\bar{v}_y = 1 \text{ (m/s)}$, $q = 0.2 \text{ (m}^2/\text{s}^3\text{)}$. The rest of the parameters of the multi-target dynamic model are $\lambda = 0.08 \text{ s}^{-1}$, $\mu = 0.01 \text{ s}^{-1}$, $\bar{x}_a = [200 \text{ (m)}, 3 \text{ (m/s)}, 250 \text{ (m)}, 0 \text{ (m/s)}]^T$ and $P_a = \text{diag}([50^2 \text{ (m}^2\text{)}, 1 \text{ (m}^2/\text{s}^2\text{)}, 50^2 \text{ (m}^2\text{)}, 1 \text{ (m}^2/\text{s}^2\text{)}])$.

The sensor takes 100 measurements. The time interval Δt_k between measurements is drawn from an exponential distribution with parameter $\mu_m = 1$ [10]. The resulting time intervals are the same as in [25, Fig. 2]. The sensor obtains position measurements with a probability of detection $p^D = 0.9$ and

$$H = \begin{bmatrix} 1 & 0 & 0 & 0 \\ 0 & 0 & 1 & 0 \end{bmatrix}, R = \sigma_r^2 I_2, \quad (85)$$

¹Matlab code is available at <https://github.com/Agarciafernandez/MTT>.

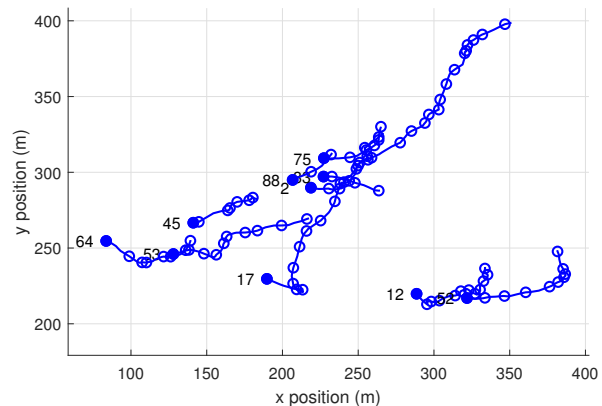


Figure 2: Ground truth set of trajectories with 10 trajectories. Every 10 time steps, the position of a trajectory is marked with circles. The initial position is marked with a filled circle, and the number next to it indicates time step of birth.

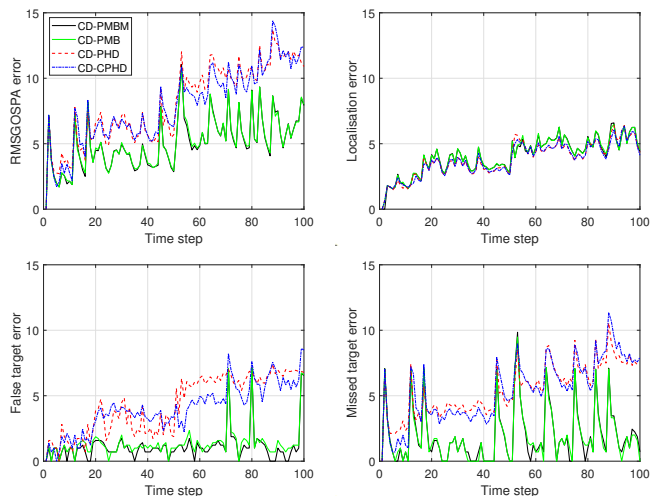


Figure 3: RMS GOSPA positional errors (m) and their decomposition against time.

where $\sigma_r^2 = 4 \text{ m}^2$. The clutter intensity is $\lambda^C(z) = 10 \cdot u_A(z)$, where $u_A(\cdot)$ is a uniform density in the area $A = [0, 600] \times [0, 400] \text{ (m}^2\text{)}$. The ground truth set of trajectories, shown in Figure 2, is drawn from the above continuous time multi-target model sampled at the sensor sampling times.

Filtering performance is evaluated via Monte Carlo simulation with 100 runs. We estimate the set of target positions and calculate its error using the generalised optimal subpattern assignment (GOSPA) metric with parameters $\alpha = 2$, $c = 10 \text{ m}$ and $p = 2$ [47]. The root mean square GOSPA (RMSGOSPA) at each time step, and its decomposition in terms of localisation errors, missed target costs and false target costs for the continuous-discrete filters are shown in Figure 3. The CD-PMBM and CD-PMB are the best performing filters. The CD-PHD and CD-CPHD have worse performance, mainly due to an increase in false target as well as missed target error.

The (discrete-time) PMBM, PMB, PHD and CPHD filters,

which consider 29374 time steps, produce very similar results to the corresponding continuous-discrete filters, so the results are not shown in Figure 3. The difference arises in the computational time. The computational times to run one Monte Carlo iteration of the filters on an Intel core i5 laptop are: 5.1 s (CD-PMBM), 1.1 s (CD-PMB), 1.5 s (CD-PHD), 2.0 s (CD-CPHD), 136.6 s (PMBM), 106.6 s (PMB), 60.1 s (PHD), 85.5 s (CPHD). We can see that the continuous-discrete filters show a noteworthy decrease in computational time compared to the discrete versions (over 26 times faster in the case of the PMBM). The reason is that the continuous-discrete filters can perform in a single step the multiple prediction steps that are required in the discrete versions.

In the following, we also analyse two simpler birth discretisation methods that approximate the single-target birth density, given by (22), as a constant across time. The first method, which we refer to as ‘‘Constant single-target birth density 1’’ (CSBD1), makes the approximation

$$p_k(x_k) \approx p_k(x_k | \hat{t}), \quad (86)$$

where \hat{t} is the expected time lag of appearance given the expected Δt_k , $E[\Delta t_k]$, which is 1 second in the simulation. Using [25, Eq. (36)], we obtain that

$$\hat{t} = \frac{1}{\mu} - \frac{E[\Delta t_k] e^{-\mu E[\Delta t_k]}}{1 - e^{-\mu E[\Delta t_k]}}. \quad (87)$$

In this scenario, $\hat{t} = 0.4992$. The second method, which we refer to as ‘‘Constant single-target birth density 2’’ (CSBD2), neglects the continuous-time effects by assuming that the single-target birth density is

$$p_k(x_k) \approx \mathcal{N}(x; \bar{x}_a, P_a). \quad (88)$$

In these implementations, the rest of the parameters of the continuous-discrete filters remain unchanged.

To notice the effect of different single-target birth discretisations, the mean and covariance matrix at the time of birth should significantly differ from those at the time of appearance. With the current appearance model, experimental results do not show a big difference between these discretisations. To show differences, we increase the mean velocity of the appearing targets to $\bar{v}_a = [20, -20]^T$ (m/s) and $\bar{v}_a = [25, -25]^T$ (m/s). For the latter velocity, we also consider an informative birth model with $P_a = I_4$, and also a constant $\Delta t_k = 1$ s.

The RMS-GOSPA errors across all time steps for the different birth models in the four considered scenarios are shown in Table II. The birth model of Prop.1 outperforms the other two variants in these cases. In particular, the improvement in performance for informative P_a is significant for both variable Δt_k and constant Δt_k . The reason is that, for informative P_a , there are important difference between the single-target birth density at the time of birth and at the time of appearance, and this has an impact in filtering performance.

B. Non-linear SDE

We consider a re-entry tracking problem [20], [48]. The state is $x(t) = [p_x(t), v_x(t), p_y(t), v_y(t)]^T$ and the SDE parameters are

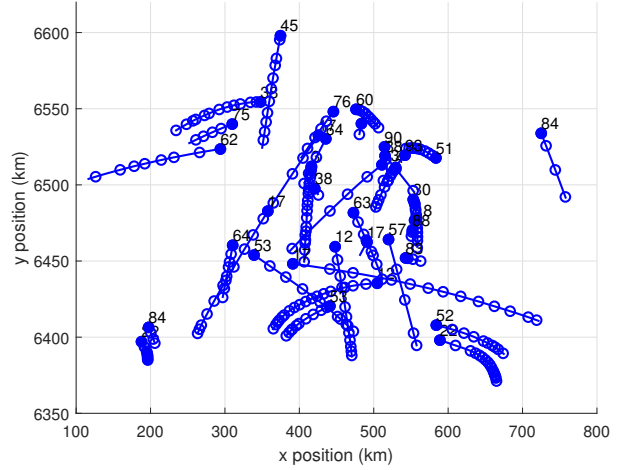


Figure 4: Ground truth set of trajectories

$$f(x) = I_2 \otimes \begin{bmatrix} 0 & 1 \\ g(x) & d(x) \end{bmatrix} x, \quad L = \begin{bmatrix} 1 \\ 1 \end{bmatrix} \otimes \begin{bmatrix} 0 & 0 \\ 1 & 0 \end{bmatrix}, \quad (89)$$

where

$$g(x) = -\frac{Gm_0}{((p_x)^2 + (p_y)^2)^{3/2}}, \quad (90)$$

$$d(x) = -\beta_0 \exp\left(\psi + \frac{r_0 - ((p_x)^2 + (p_y)^2)^{1/2}}{h_0}\right) \times \sqrt{(v_x)^2 + (v_y)^2}, \quad (91)$$

where $Gm_0 = 3.986 \cdot 10^5 \text{ km}^3/\text{s}^2$, $\beta_0 = 0.6 \text{ km}^{-1}$, $\psi = 0.7$ is an aerodynamic parameter, $r_0 = 6374 \text{ km}$, $h_0 = 13.4 \text{ km}$ where $Q_\beta = 10^{-4} I_2$. Targets appear with $\bar{x}_a = [450 \text{ (km)}, -0.1 \text{ (km/s)}, 6500 \text{ (km)}, -1 \text{ (km/s)}]^T$ and $P_a =$

$$\text{diag}([100^2 \text{ (km}^2\text{)}, 3^2 \text{ (km}^2/\text{s}^2\text{)}, 50^2 \text{ (km}^2\text{)}, 1 \text{ (km}^2/\text{s}^2\text{)}]).$$

The parameters that model the appearance and disappearance times of targets are $\lambda = 0.3 \text{ s}^{-1}$ and $\mu = 0.01 \text{ s}^{-1}$.

As in the previous scenario, the sensor takes 100 measurements with the same time interval Δt_k between measurements. The sensor measures positions with $p^D = 0.9$ and matrices (85) with $\sigma_r^2 = 10^{-2} \text{ km}^2$. The clutter intensity is $\lambda^C(z) = 10u_A(z)$ with area $A = [0, 900] \times [0, 6600]$ (km^2).

We sample the ground truth set of trajectories at the sensor sampling times using an Euler-Maruyama method to simulate the trajectories from the ODEs with a step-size of 0.01 s [8, Alg. 8.1]. The resulting set of trajectories is shown in Figure 4. The parameters of the GOSPA metric in this scenario are $\alpha = 2$, $c = 0.1 \text{ km}$ and $p = 2$. The RMS-GOSPA error and its decomposition at each time step are shown in Figure 5. CD-PMBM and CD-PMB filters have the best performance. The worse performance of CD-PHD and CD-CPHD filters is mainly due to an increase in the number of missed targets, though these filters also usually report a higher number of false targets.

Table II: RMS-GOSPA error (m) across all time steps for different single-target birth discretisations in the linear SDE example

Birth	$\bar{v}_a = [20, -20]^T$			$\bar{v}_a = [25, -25]^T$			$\bar{v}_a = [25, -25]^T, P_a = I_4$			$\bar{v}_a = [25, -25]^T, P_a = I_4, \Delta t_k = 1s$		
	Prop. 1	CSBD1	CSBD2	Prop. 1	CSBD1	CSBD2	Prop. 1	CSBD1	CSBD2	Prop. 1	CSBD1	CSBD2
CD-PMBM	5.43	5.47	5.51	5.43	5.47	5.54	4.94	6.38	9.12	4.92	5.55	5.62
CD-PMB	5.46	5.48	5.54	5.46	5.50	5.53	5.04	6.24	9.14	4.95	5.57	5.60
CD-PHD	8.77	9.17	9.41	8.83	9.34	9.74	8.26	9.23	10.28	8.38	9.46	9.50
CD-CPHD	8.45	8.80	9.14	8.48	9.12	9.61	8.16	9.37	10.75	8.26	9.61	9.64

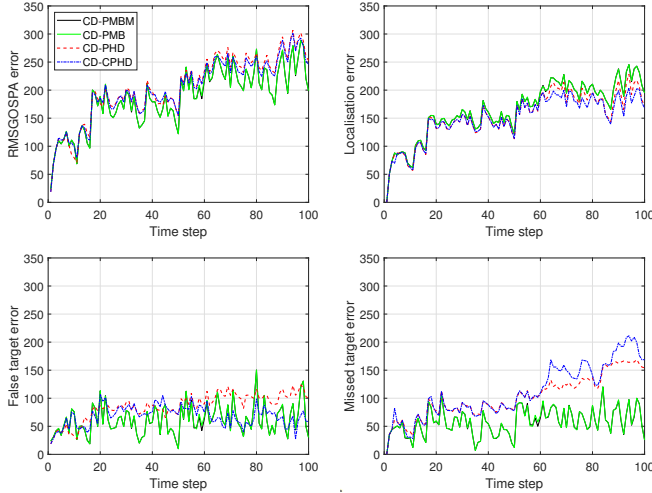


Figure 5: RMS GOSPA positional errors (m) and their decomposition against time.

As in the linear case, the PMBM, PMB, PHD and CPHD filters have very similar errors to the corresponding continuous-discrete filters, so the results are not shown in Figure 5. The computational times to run one Monte Carlo iteration of the filters on an Intel core i5 laptop are: 2.6 s (CD-PMBM), 2.4 s (CD-PMB), 3.3 s (CD-PHD), 3.3 s (CD-CPHD), 9424.1 s (PMBM), 8800.4 s (PMB), 307.3 s (PHD), 319.6 s (CPHD). The continuous-discrete filters are remarkably faster than the discrete filters. For instance, the CD-PMBM filter is over 3500 times faster than the PMBM filter.

The results for the different single-target birth density discretisations, explained in Section V-A, are quite similar in this scenario. As in the previous scenario, we analyse the effect for higher mean appearing velocities $\bar{v}_a = [10, -10]^T$ (km/s) and $\bar{v}_a = [15, -15]^T$ (km/s), and also for an informative birth density $P_a = I_4$, and also a constant $\Delta t_k = 1s$.

Table III shows the RMS-GOSPA error across all time steps for the different single-target birth density discretisations in the four considered scenarios. As before, the birth discretisation of Prop. 8 outperforms the other two discretisations. The improvement is more significant in the informative birth cases.

VI. CONCLUSIONS

This paper has derived the Gaussian implementation of the continuous-discrete Poisson multi-Bernoulli mixture filter, which computes the filtering density when target appearance, dynamics and disappearance are in continuous time, and measurements are taken at discrete time steps. We have derived the single-target transition density and the best Gaussian fit, obtained via moment matching, to the single-target birth distribution when dynamics are modelled by linear, time-invariant

SDEs. We have also derived the steady-state birth density, and the corresponding filter simplification.

The results have been extended to non-linear, time-invariant SDEs. These yield the continuous-discrete versions of the PMBM, PMB, PHD and CPHD filters. For non-uniform sampling intervals, the developed continuous-discrete filters show similar estimation error with a remarkable decrease in computational time compared to analogous discrete filters with uniform sampling time.

There are many lines of possible future research based on this work, for example, the derivation of continuous-discrete PMBM filters using the exponential family of distributions [49] or Gaussian mixtures [50], and the use of variational techniques for continuous-discrete multi-target filtering.

REFERENCES

- [1] S. Challa, M. R. Morelande, D. Musicki, and R. J. Evans, *Fundamentals of Object Tracking*. Cambridge University Press, 2011.
- [2] F. Meyer, T. Kropfreiter, J. L. Williams, R. Lau, F. Hlawatsch, P. Braca, and M. Z. Win, "Message passing algorithms for scalable multitarget tracking," *Proceedings of the IEEE*, vol. 106, no. 2, pp. 221–259, Feb. 2018.
- [3] J. Houssineau and D. E. Clark, "Multitarget filtering with linearized complexity," *IEEE Transactions on Signal Processing*, vol. 66, no. 18, pp. 4957–4970, Sept. 2018.
- [4] E. Delande, J. Houssineau, J. Franco, C. Frueh, D. Clark, and M. Jah, "A new multi-target tracking algorithm for a large number of orbiting objects," *Advances in Space Research*, vol. 64, pp. 645–667, 2019.
- [5] S. Pang and H. Radha, "Multi-object tracking using Poisson multi-Bernoulli mixture filtering for autonomous vehicles," in *IEEE International Conference on Acoustics, Speech and Signal Processing*, 2021, pp. 7963–7967.
- [6] D. K. M. Kufoalor, T. A. Johansen, E. F. Brekke, A. Hepsø, and K. Trmka, "Autonomous maritime collision avoidance: Field verification of autonomous surface vehicle behavior in challenging scenarios," *Journal of Field Robotics*, vol. 37, no. 3, 2020.
- [7] M. Lambert, S. r. Bonnabel, and F. Bach, "The continuous-discrete variational Kalman filter (CD-VKF)," in *IEEE 61st Conference on Decision and Control*, 2022, pp. 6632–6639.
- [8] S. Särkkä and A. Solin, *Applied Stochastic Differential Equations*. Cambridge University Press, 2019.
- [9] Y. Hu, Z. Duan, and D. Zhou, "Estimation fusion with general asynchronous multi-rate sensors," *IEEE Transactions on Aerospace and Electronic Systems*, vol. 46, no. 4, pp. 2090–2102, 2010.
- [10] F. Eng, "Non-uniform sampling in statistical signal processing," Ph.D. dissertation, Linköping University, 2007.
- [11] X. Zhang, P. Willett, and Y. Bar-Shalom, "Uniform versus nonuniform sampling when tracking in clutter," *IEEE Transactions on Aerospace and Electronic Systems*, vol. 42, no. 2, pp. 388–400, 2006.
- [12] X. Ge, Q.-L. Han, X.-M. Zhang, L. Ding, and F. Yang, "Distributed event-triggered estimation over sensor networks: A survey," *IEEE Transactions on Cybernetics*, vol. 50, no. 3, pp. 1306–1320, 2020.
- [13] M. ney, L. M. Millefiori, and P. Braca, "Data driven vessel trajectory forecasting using stochastic generative models," in *IEEE International Conference on Acoustics, Speech and Signal Processing (ICASSP)*, 2019, pp. 8459–8463.
- [14] B. Øksendal, *Stochastic Differential Equations: An Introduction with Applications*. Springer-Verlag, 2003.
- [15] X. Li and V. Jilkov, "Survey of maneuvering target tracking. Part I: Dynamic models," *IEEE Transactions on Aerospace and Electronic Systems*, vol. 39, no. 4, pp. 1333–1364, Oct. 2003.

Table III: RMS-GOSPA error (m) across all time steps for different single-target birth discretisations in the non-linear SDE example

Birth	$\bar{v}_a = [10, -10]^T$			$\bar{v}_a = [15, -15]^T$			$\bar{v}_a = [15, -15]^T, P_a = I_4$			$\bar{v}_a = [15, -15]^T, P_a = I_4, \Delta t_k = 1s$		
	Prop. 8	CSBD1	CSBD2	Prop. 8	CSBD1	CSBD2	Prop. 8	CSBD1	CSBD2	Prop. 8	CSBD1	CSBD2
CD-PMBM	194.40	196.11	196.14	199.69	199.89	200.15	184.99	219.84	230.59	186.32	208.24	214.85
CD-PMB	193.71	195.56	195.62	199.68	199.86	200.11	185.17	220.82	231.28	186.82	208.99	214.88
CD-PHD	218.82	218.96	219.17	221.61	221.54	221.90	214.98	232.66	235.51	215.32	229.89	229.70
CD-CPHD	219.31	219.46	219.28	222.41	222.35	222.43	215.16	230.75	234.77	214.35	228.93	228.08

- [16] L. M. Millefiori, P. Braca, and P. Willett, "Consistent estimation of randomly sampled Ornstein-Uhlenbeck process long-run mean for long-term target state prediction," *IEEE Signal Processing Letters*, vol. 23, no. 11, pp. 1562–1566, Nov. 2016.
- [17] L. M. Millefiori, P. Braca, K. Bryan, and P. Willett, "Modeling vessel kinematics using a stochastic mean-reverting process for long-term prediction," *IEEE Transactions on Aerospace and Electronic Systems*, vol. 52, no. 5, pp. 2313–2330, Oct. 2016.
- [18] S. Coraluppi and C. Carthel, "Stability and stationarity in target kinematic modeling," in *IEEE Aerospace Conference*, 2012, pp. 1–8.
- [19] M. Morelande and N. Gordon, "Target tracking through a coordinated turn," in *Proceedings of IEEE International Conference on Acoustics, Speech, and Signal Processing*, vol. 4, 2005, pp. 21–24.
- [20] F. Tronarp and S. S. rkk, "Iterative statistical linear regression for Gaussian smoothing in continuous-time non-linear stochastic dynamic systems," *Signal Processing*, vol. 159, pp. 1–12, June 2019.
- [21] P. Axelsson and F. Gustafsson, "Discrete-time solutions to the continuous-time differential Lyapunov equation with applications to Kalman filtering," *IEEE Transactions on Automatic Control*, vol. 60, no. 3, pp. 632–643, March 2015.
- [22] C. Van Loan, "Computing integrals involving the matrix exponential," *IEEE Transactions on Automatic Control*, vol. 23, no. 3, pp. 395–404, 1978.
- [23] S. Särkkä and A. Solin, "On continuous-discrete cubature Kalman filtering," in *16th IFAC Symposium on System Identification*, 2012, pp. 1221–1226.
- [24] I. Arasaratnam, S. Haykin, and T. Hurd, "Cubature Kalman filtering for continuous-discrete systems: Theory and simulations," *IEEE Transactions on Signal Processing*, vol. 58, no. 10, pp. 4977–4993, Oct. 2010.
- [25] A. F. García-Fernández and S. Maskell, "Continuous-discrete multiple target filtering: PMBM, PHD and CPHD filter implementations," *IEEE Transactions on Signal Processing*, vol. 68, pp. 1300–1314, 2020.
- [26] A. F. García-Fernández and W. Yi, "Continuous-discrete multiple target tracking with out-of-sequence measurements," *IEEE Transactions on Signal Processing*, vol. 69, pp. 4699–4709, 2021.
- [27] S. Coraluppi and C. A. Carthel, "If a tree falls in the woods, it does make a sound: multiple-hypothesis tracking with undetected target births," *IEEE Transactions on Aerospace and Electronic Systems*, vol. 50, no. 3, pp. 2379–2388, July 2014.
- [28] L. Kleinrock, *Queueing Systems*. John Wiley & Sons, 1976.
- [29] J. L. Williams, "Marginal multi-Bernoulli filters: RFS derivation of MHT, JIPDA and association-based MeMBer," *IEEE Transactions on Aerospace and Electronic Systems*, vol. 51, no. 3, pp. 1664–1687, July 2015.
- [30] A. F. García-Fernández, J. L. Williams, K. Granström, and L. Svensson, "Poisson multi-Bernoulli mixture filter: direct derivation and implementation," *IEEE Transactions on Aerospace and Electronic Systems*, vol. 54, no. 4, pp. 1883–1901, Aug. 2018.
- [31] E. Brekke and M. Chitre, "Relationship between finite set statistics and the multiple hypothesis tracker," *IEEE Transactions on Aerospace and Electronic Systems*, vol. 54, no. 4, pp. 1902–1917, Aug. 2018.
- [32] P. Bostrom-Rost, D. Axehill, and G. Hendeby, "Sensor management for search and track using the Poisson multi-Bernoulli mixture filter," *IEEE Transactions on Aerospace and Electronic Systems*, vol. 57, no. 5, pp. 2771–2783, 2021.
- [33] J. T. Horwood, N. D. Aragon, and A. B. Poore, "Gaussian sum filters for space surveillance: Theory and simulations," *Journal of Guidance, Control and Dynamics*, vol. 34, pp. 1839–1851, 2011.
- [34] D. Crouse, "Basic tracking using nonlinear continuous-time dynamic models [tutorial]," *IEEE Aerospace and Electronic Systems Magazine*, vol. 30, no. 2, pp. 4–41, 2015.
- [35] R. P. S. Mahler, *Advances in Statistical Multisource-Multitarget Information Fusion*. Artech House, 2014.
- [36] A. F. García-Fernández, L. Svensson, J. L. Williams, Y. Xia, and K. Granström, "Trajectory Poisson multi-Bernoulli filters," *IEEE Transactions on Signal Processing*, vol. 68, pp. 4933–4945, 2020.
- [37] J. L. Williams, "An efficient, variational approximation of the best fitting multi-Bernoulli filter," *IEEE Transactions on Signal Processing*, vol. 63, no. 1, pp. 258–273, Jan. 2015.
- [38] A. F. García-Fernández and B.-N. Vo, "Derivation of the PHD and CPHD filters based on direct Kullback-Leibler divergence minimization," *IEEE Transactions on Signal Processing*, vol. 63, no. 21, pp. 5812–5820, Nov. 2015.
- [39] F. Carbonell, J. C. J. menez, and L. M. Pedroso, "Computing multiple integrals involving matrix exponentials," *Journal of Computational and Applied Mathematics*, vol. 213, pp. 300–305, 2008.
- [40] V. G. Kulkarni, *Modeling and analysis of stochastic systems*. Chapman & Hall/CRC, 2016.
- [41] J. Hershey and P. Olsen, "Approximating the Kullback Leibler divergence between Gaussian mixture models," in *IEEE International Conference on Acoustics, Speech and Signal Processing*, vol. 4, April 2007, pp. 317–320.
- [42] G. H. Golub and C. F. Van Loan, *Matrix computations*. The Johns Hopkins University Press, 1996.
- [43] H. K. Khalil, *Nonlinear systems*. Prentice Hall, 2002.
- [44] B.-N. Vo and W.-K. Ma, "The Gaussian mixture probability hypothesis density filter," *IEEE Transactions on Signal Processing*, vol. 54, no. 11, pp. 4091–4104, Nov. 2006.
- [45] B.-T. Vo, B.-N. Vo, and A. Cantoni, "Analytic implementations of the cardinalized probability hypothesis density filter," *IEEE Transactions on Signal Processing*, vol. 55, no. 7, pp. 3553–3567, July 2007.
- [46] K. Granström, M. Fatemi, and L. Svensson, "Poisson multi-Bernoulli mixture conjugate prior for multiple extended target filtering," *IEEE Transactions on Aerospace and Electronic Systems*, vol. 56, no. 1, pp. 208–225, Feb. 2020.
- [47] A. S. Rahmathullah, A. F. G. a Fern ndez, and L. Svensson, "Generalized optimal sub-pattern assignment metric," in *20th International Conference on Information Fusion*, 2017, pp. 1–8.
- [48] S. J. Julier and J. K. Uhlmann, "Unscented filtering and nonlinear estimation," *Proceedings of the IEEE*, vol. 92, no. 3, pp. 401–422, Mar. 2004.
- [49] D. Brigo, B. Hanzon, and F. Le Gland, "Approximate nonlinear filtering by projection on exponential manifolds of densities," *Bernoulli*, vol. 5, no. 3, pp. 495–534, 1999.
- [50] M. Lambert, S. Chewi, F. Bach, S. re Bonnabel, and P. Rigollet, "Variational inference via Wasserstein gradient flows," in *36th Conference on Neural Information Processing Systems*, 2022, pp. 1–14.
- [51] B. C. Hall, *Lie groups, Lie algebras, and representations: An elementary introduction*. Springer, 2015.
- [52] S. Ross, *A First Course in Probability*, 8th ed. Prentice-Hall, 2010.
- [53] T. M. Apostol, *Calculus. Volume I*. John Wiley & Sons, 1967.

Supplemental material: “Gaussian multi-target filtering with target dynamics driven by a stochastic differential equation”

APPENDIX A

In this appendix we prove (10). For the given H_c^3 in (12), the value of $H_1(t)$ in (11) is given by [22, Sec. II]

$$\begin{aligned} H_1(t) &= \int_0^t \int_0^s \exp(-B(t-s)) Q_c \exp(Ar) dr ds \\ &= \exp(-Bt) \int_0^t \exp(Bs) Q_c \left(\int_0^s \exp(Ar) dr \right) ds. \end{aligned} \quad (92)$$

Therefore, by using the property that, for a square matrix X [51],

$$\exp(-X) = (\exp(X))^{-1}, \quad (93)$$

and multiplying by the inverse of $\exp(-Bt)$ on the left for both sides of the equation in (92), we complete the proof of (10).

APPENDIX B

In this appendix, we prove Proposition 1. We prove the mean in Section B-A and the covariance matrix in Section B-B.

It should be noted that (24) and (28) are obtained by the law of total expectation and the law of total covariance, respectively [52]. In the proofs, we will use this result. Given two $n_x \times n_x$ matrices X and Y such that $XY = YX$, then [51]

$$\exp(X) \exp(Y) = \exp(X + Y). \quad (94)$$

A. Mean

Plugging (21) and (19) into (24) yields

$$\bar{x}_{b,k} = \bar{x}_{b,k,1} + \bar{x}_{b,k,2}, \quad (95)$$

where

$$\bar{x}_{b,k,1} = \frac{\mu}{1 - e^{-\mu\Delta t_k}} \int_0^{\Delta t_k} \exp(At) \bar{x}_a e^{-\mu t} dt, \quad (96)$$

$$\bar{x}_{b,k,2} = \frac{\mu}{1 - e^{-\mu\Delta t_k}} \int_0^{\Delta t_k} \left[\int_0^t \exp(A\tau) d\tau \right] u e^{-\mu t} dt. \quad (97)$$

We proceed to calculate (96) and (97).

1) *Calculation of (96)*: Operating on (96), we obtain

$$\begin{aligned} \bar{x}_{b,k,1} &= \frac{\mu}{1 - e^{-\mu\Delta t_k}} \left[\int_0^{\Delta t_k} \exp(At) e^{-\mu t} I dt \right] \bar{x}_a \\ &= \frac{\mu}{1 - e^{-\mu\Delta t_k}} \left[\int_0^{\Delta t_k} \exp(At) e^{-\mu t} dt \right] \bar{x}_a. \end{aligned} \quad (98)$$

We know that $At \times \mu I_{n_x} t = \mu I_{n_x} t \times At$, then we can apply (94) to obtain

$$\bar{x}_{b,k,1} = \frac{\mu}{1 - e^{-\mu\Delta t_k}} \left[\int_0^{\Delta t_k} \exp((A - \mu I) t) dt \right] \bar{x}_a. \quad (99)$$

Making use of (5) yields

$$\bar{x}_{b,k,1} = \frac{\mu}{1 - e^{-\mu\Delta t_k}} \begin{bmatrix} I & 0_{n_x,1} \end{bmatrix} \exp(\bar{A}_b \Delta t_k) \begin{bmatrix} 0_{n_x,1} \\ 1 \end{bmatrix}, \quad (100)$$

where \bar{A}_b is given by (26).

2) *Calculation of (97)*: We first calculate the inner integral in (97). Using (5), we obtain

$$\int_0^t \exp(A\tau) d\tau u = \begin{bmatrix} I & 0_{n_x,1} \end{bmatrix} \exp(\bar{A}_{b,u,1} t) \begin{bmatrix} 0_{n_x,1} \\ 1 \end{bmatrix}, \quad (101)$$

where

$$\bar{A}_{b,u,1} = \begin{bmatrix} A & u \\ 0_{1,n_x} & 0 \end{bmatrix}. \quad (102)$$

Substituting this expression into (97) yields

$$\begin{aligned} \bar{x}_{b,k,2} &= \frac{\mu}{1 - e^{-\mu\Delta t_k}} \begin{bmatrix} I & 0_{n_x,1} \end{bmatrix} \\ &\quad \times \int_0^{\Delta t_k} \exp(\bar{A}_{b,u,1} t) e^{-\mu t} dt \begin{bmatrix} 0_{n_x,1} \\ 1 \end{bmatrix}. \end{aligned} \quad (103)$$

We calculate the following integral using the approach in Section B-A1

$$\begin{aligned} &\int_0^{\Delta t_k} \exp(\bar{A}_{b,u,1} t) e^{-\mu t} dt \begin{bmatrix} 0_{n_x,1} \\ 1 \end{bmatrix} \\ &= \int_0^{\Delta t_k} \exp((\bar{A}_{b,u,1} - \mu I_{n_x+1}) t) dt \begin{bmatrix} 0_{n_x,1} \\ 1 \end{bmatrix} \\ &= \int_0^{\Delta t_k} \exp\left(\begin{bmatrix} A - \mu I & u \\ 0_{1,n_x} & -\mu \end{bmatrix} t\right) dt \begin{bmatrix} 0_{n_x,1} \\ 1 \end{bmatrix}, \end{aligned} \quad (104)$$

where I_{n_x+1} is an identity matrix of size $n_x + 1$.

Making use of (5), we obtain

$$\begin{aligned} \bar{x}_{b,k,2} &= \frac{\mu}{1 - e^{-\mu\Delta t_k}} \begin{bmatrix} I & 0_{n_x,1} \end{bmatrix} \begin{bmatrix} I_{n_x+1} & 0_{n_x+1,1} \end{bmatrix} \\ &\quad \times \exp(\bar{A}_{b,u,2} t) \begin{bmatrix} 0_{n_x+1,1} \\ 1 \end{bmatrix} \\ &= \frac{\mu}{1 - e^{-\mu\Delta t_k}} \begin{bmatrix} I & 0_{n_x,2} \end{bmatrix} \exp(\bar{A}_{b,u} t) \begin{bmatrix} 0_{n_x+1,1} \\ 1 \end{bmatrix}, \end{aligned} \quad (105)$$

where $\bar{A}_{b,u}$ is given by (27). The calculated values of $\bar{x}_{b,k,1}$ and $\bar{x}_{b,k,2}$ finish the proof of (25).

B. Term $E[C[x_k|t]]$

We proceed to prove $E[C[x_k|t]]$ in (28). Using (21) and (20), we write

$$E[C[x_k|t]] = E_1 + E_2, \quad (106)$$

where

$$E_1 = E \left[\int_0^t \exp(A\tau) LQ_\beta L^T \exp(A^T \tau) d\tau \right],$$

$$= \frac{\mu}{1 - e^{-\mu\Delta t_k}} \int_0^{\Delta t_k} e^{-\mu t} \quad (107)$$

$$\times \left[\int_0^t \exp(A\tau) LQ_\beta L^T \exp(A^T \tau) d\tau \right] dt, \quad (108)$$

and

$$E_2 = E \left[\exp(At) P_a \exp(A^T t) \right],$$

$$= \frac{\mu}{1 - e^{-\mu\Delta t_k}} \int_0^{\Delta t_k} \exp(At) P_a \exp(A^T t) e^{-\mu t} dt. \quad (109)$$

We first calculate E_1 and then proceed to calculate (106).

1) Term E_1 : We calculate (108) by integrating by parts [53]. We define

$$u(t) = \frac{\mu}{1 - e^{-\mu\Delta t_k}} \int_0^t \exp(A\tau) LQ_\beta L^T \exp(A^T \tau) d\tau,$$

$$v'(t) dt = e^{-\mu t} dt,$$

which implies

$$u'(t) dt = \frac{\mu}{1 - e^{-\mu\Delta t_k}} \exp(At) LQ_\beta L^T \exp(A^T t) dt,$$

$$v(t) = -\frac{e^{-\mu t}}{\mu}.$$

Then,

$$E_1 = \frac{1}{1 - e^{-\mu\Delta t_k}} \left[-e^{-\mu\Delta t_k} \right.$$

$$\times \int_0^{\Delta t_k} \exp(A\tau) LQ_\beta L^T \exp(A^T \tau) d\tau$$

$$\left. + \int_0^{\Delta t_k} e^{-\mu\tau} \exp(A\tau) LQ_\beta L^T \exp(A^T \tau) d\tau \right]. \quad (110)$$

2) Rest of the proof: Substituting (110) and (109) into (106), we obtain

$$E[C[x_k|t]]$$

$$= -\frac{e^{-\mu\Delta t_k}}{1 - e^{-\mu\Delta t_k}} \int_0^{\Delta t_k} \exp(A\tau) LQ_\beta L^T \exp(A^T \tau) d\tau$$

$$+ \frac{1}{1 - e^{-\mu\Delta t_k}} \int_0^{\Delta t_k} e^{-\mu\tau} \exp(A\tau) C_b \exp(A^T \tau) d\tau, \quad (111)$$

where C_b is given by (31). The first integral in (111) can be calculated using (7). Following the procedure in Section B-A1, the second integral in (111) can be written as

$$\int_0^{\Delta t_k} e^{-\mu t} \exp(At) C_b \exp(A^T t) dt$$

$$= \int_0^{\Delta t_k} \exp((A - \mu/2I)t) C_b \exp((A - \mu/2I)^T t) dt. \quad (112)$$

Integral (112) can be computed using (7). This proves the expression for $E[C[x_k|t]]$ in Proposition 1.

C. Term $C[E[x_k|t]]$

We expand $C[E[x_k|t]]$ as

$$C[E[x_k|t]] = E \left[E[x_k|t] E[x_k|t]^T \right] - \bar{x}_{b,k} \bar{x}_{b,k}^T. \quad (113)$$

Substituting (19) into $E \left[E[x_k|t] E[x_k|t]^T \right]$, we obtain

$$E \left[E[x_k|t] E[x_k|t]^T \right]$$

$$= E \left[\left(\exp(At) \bar{x}_a + \int_0^t \exp(A\tau) d\tau u \right) \right.$$

$$\times \left(\bar{x}_a^T \exp(A^T t) + u^T \int_0^t \exp(A^T \tau) d\tau \right) \left. \right]$$

$$= E \left[\exp(At) \bar{x}_a \bar{x}_a^T \exp(A^T t) \right]$$

$$+ E \left[\exp(At) \bar{x}_a u^T \left(\int_0^t \exp(A^T \tau) d\tau \right) \right]$$

$$+ E \left[\int_0^t \exp(A\tau) d\tau u \bar{x}_a^T \exp(A^T t) \right]$$

$$+ E \left[\int_0^t \exp(A\tau) d\tau u u^T \int_0^t \exp(A^T \tau) d\tau \right]. \quad (114)$$

We proceed to calculate the required integrals in (114). The first type of integral in (114) is

$$\Sigma_{xx} = E \left[\exp(At) \bar{x}_a \bar{x}_a^T \exp(A^T t) \right]$$

$$= \frac{\mu}{1 - e^{-\mu\Delta t_k}} \int_0^{\Delta t_k} \exp(At) \bar{x}_a \bar{x}_a^T \exp(A^T t) e^{-\mu t} dt$$

$$= \frac{\mu}{1 - e^{-\mu\Delta t_k}} \int_0^{\Delta t_k} \exp((A - \mu/2I)t) \bar{x}_a \bar{x}_a^T$$

$$\times \exp((A - \mu/2I)^T t) dt. \quad (115)$$

This is an integral of the form (7) that we can calculate.

The second type of integral in (114) is

$$\Sigma_{xu} = E \left[\exp(At) \bar{x}_a u^T \left(\int_0^t \exp(A^T \tau) d\tau \right) \right]$$

$$= \frac{\mu}{1 - e^{-\mu\Delta t_k}} \int_0^{\Delta t_k} \exp(At) \bar{x}_a u^T$$

$$\times \left(\int_0^t \exp(A^T \tau) d\tau \right) e^{-\mu t} dt$$

$$= \frac{\mu}{1 - e^{-\mu\Delta t_k}} \int_0^{\Delta t_k} \exp((A - \mu I)t) \bar{x}_a u^T$$

$$\times \left(\int_0^t \exp(A^T \tau) d\tau \right) dt. \quad (116)$$

This is an integral of the form (10) that we can calculate.

The third type of integral in (114) is

$$\Sigma_{uu} = E \left[\int_0^t \exp(A\tau) d\tau u u^T \int_0^t \exp(A^T \tau) d\tau \right]$$

$$\begin{aligned}
&= \frac{\mu}{1 - e^{-\mu\Delta t_k}} \int_0^{\Delta t_k} e^{-\mu t} \\
&\times \left[\int_0^t \exp(A\tau) d\tau uu^T \int_0^t \exp(A^T\tau) d\tau \right] dt. \quad (117)
\end{aligned}$$

1) *Integration by parts for Σ_{uu}* : We compute (117) by parts. We define

$$u(t) = \frac{\mu}{1 - e^{-\mu\Delta t_k}} \int_0^t \exp(A\tau) d\tau uu^T \int_0^t \exp(A^T\tau) d\tau, \quad (118)$$

$$v'(t)dt = e^{-\mu t} dt, \quad (119)$$

which implies

$$\begin{aligned}
u'(t)dt &= \frac{\mu}{1 - e^{-\mu\Delta t_k}} \left[\exp(At) uu^T \left(\int_0^t \exp(A^T\tau) d\tau \right) \right. \\
&\quad \left. + \left(\int_0^t \exp(A\tau) d\tau \right) uu^T \exp(A^T t) \right], \quad (120)
\end{aligned}$$

$$v(t) = -\frac{e^{-\mu t}}{\mu}. \quad (121)$$

Then, we have

$$\begin{aligned}
\Sigma_{uu} &= -\frac{\mu}{1 - e^{-\mu\Delta t_k}} \\
&\times \left[\int_0^t \exp(A\tau) d\tau uu^T \int_0^t \exp(A^T\tau) d\tau \frac{e^{-\mu t}}{\mu} \right]_0^{\Delta t_k} \\
&+ \frac{\mu}{1 - e^{-\mu\Delta t_k}} \int_0^{\Delta t_k} \frac{e^{-\mu t}}{\mu} \\
&\times \left[\exp(At) uu^T \left(\int_0^t \exp(A^T\tau) d\tau \right) \right. \\
&= -\frac{\mu}{1 - e^{-\mu\Delta t_k}} \left[\frac{e^{-\mu\Delta t_k}}{\mu} \int_0^{\Delta t_k} \exp(A\tau) d\tau uu^T \right. \\
&\times \left. \int_0^{\Delta t_k} \exp(A^T\tau) d\tau \right] \\
&+ \frac{\mu}{1 - e^{-\mu\Delta t_k}} \int_0^{\Delta t_k} \exp(At) uu^T \\
&\times \left(\int_0^t \exp(A^T\tau) d\tau \right) \frac{e^{-\mu t}}{\mu} dt \\
&+ \frac{\mu}{1 - e^{-\mu\Delta t_k}} \int_0^{\Delta t_k} \left(\int_0^t \exp(A\tau) d\tau \right) uu^T \\
&\times \exp(A^T t) \frac{e^{-\mu t}}{\mu} dt \\
&= -\frac{e^{-\mu\Delta t_k}}{1 - e^{-\mu\Delta t_k}} \int_0^{\Delta t_k} \exp(A\tau) d\tau uu^T \\
&\times \int_0^{\Delta t_k} \exp(A^T\tau) d\tau \\
&+ \frac{1}{1 - e^{-\mu\Delta t_k}} \int_0^{\Delta t_k} \exp(At) uu^T \\
&\times \left(\int_0^t \exp(A^T\tau) d\tau \right) e^{-\mu t} dt \\
&+ \frac{1}{1 - e^{-\mu\Delta t_k}} \int_0^{\Delta t_k} \left(\int_0^t \exp(A\tau) d\tau \right) uu^T
\end{aligned}$$

$$\begin{aligned}
&\times \exp(A^T t) e^{-\mu t} dt \\
&= -\frac{e^{-\mu\Delta t_k}}{1 - e^{-\mu\Delta t_k}} \int_0^{\Delta t_k} \exp(A\tau) d\tau uu^T \\
&\times \int_0^{\Delta t_k} \exp(A^T\tau) d\tau \\
&+ \frac{1}{1 - e^{-\mu\Delta t_k}} \int_0^{\Delta t_k} \exp((A - \mu I)t) uu^T \\
&\times \left(\int_0^t \exp(A^T\tau) d\tau \right) dt \\
&+ \frac{1}{1 - e^{-\mu\Delta t_k}} \int_0^{\Delta t_k} \left(\int_0^t \exp(A\tau) d\tau \right) uu^T \\
&\times \exp((A - \mu I)^T t) dt. \quad (122)
\end{aligned}$$

This proves (30) and completes the proof of Proposition 1.

APPENDIX C

In this appendix, we prove Lemma 3. We first prove the mean and then the covariance matrix.

A. Mean

Substituting (38) into (19) yields

$$\mathbb{E}[x_k | t] = -\exp(At) A^{-1}u + \int_0^t \exp(A\tau) d\tau u. \quad (123)$$

As A is invertible, we have that

$$\begin{aligned}
\mathbb{E}[x_k | t] &= -\exp(At) A^{-1}u + [\exp(At) - I] A^{-1}u \\
&= -A^{-1}u. \\
&= x_\infty. \quad (124)
\end{aligned}$$

Then, it is direct to obtain that

$$\begin{aligned}
\bar{x}_{b,k} &= \mathbb{E}[\mathbb{E}[x_k | t]] \\
&= x_\infty. \quad (125)
\end{aligned}$$

This proves the result for the mean.

B. Covariance matrix

Substituting (39) into (20)

$$\begin{aligned}
C[x_k | t] &= \exp(At) P_\infty \exp(A^T t) \\
&\quad + \int_0^t \exp(A\tau) LQ_\beta L^T \exp(A^T\tau) d\tau \\
&= \exp(At) \left[\int_0^\infty \exp(A\tau) LQ_\beta L^T \exp(A^T\tau) d\tau \right] \\
&\quad \times \exp(A^T t) \\
&\quad + \int_0^t \exp(A\tau) LQ_\beta L^T \exp(A^T\tau) d\tau \\
&= \int_0^\infty \exp(A(t + \tau)) LQ_\beta L^T \exp(A^T(t + \tau)) d\tau \\
&\quad + \int_0^t \exp(A\tau) LQ_\beta L^T \exp(A^T\tau) d\tau. \quad (126)
\end{aligned}$$

Making the change of variable $l = \tau + t$ in the first integral, we obtain

$$\begin{aligned} C[x_k | t] &= \int_t^\infty \exp(Al) LQ_\beta L^T \exp(A^T l) dl \\ &\quad + \int_0^t \exp(A\tau) LQ_\beta L^T \exp(A^T \tau) d\tau \\ &= \int_0^\infty \exp(A\tau) LQ_\beta L^T \exp(A^T \tau) d\tau \\ &= P_\infty. \end{aligned} \quad (127)$$

Then, it is direct to obtain that

$$\begin{aligned} P_{b,k} &= C[E[x_k | t]] + E[C[x_k | t]] \\ &= 0 + P_\infty. \end{aligned} \quad (128)$$

This finishes the proof of Lemma 3.

APPENDIX D

In this appendix, we prove Lemma 7. We first prove (71) and then (72).

A. Proof of (71)

Using (69) and (70) and the conditions in Lemma 7, the predicted mean number of undetected targets is

$$\bar{\lambda}_{k|k-1} = p^S (1 - p^D) \bar{\lambda}_{k-1|k-2} + \bar{\lambda}^B. \quad (129)$$

In the steady-state solution, $\bar{\lambda}_{k|k-1} = \bar{\lambda}_{k-1|k-2} = \bar{\lambda}_{k|k-1}^\infty$, which yields

$$\bar{\lambda}_{k|k-1}^\infty = p^S (1 - p^D) \bar{\lambda}_{k|k-1}^\infty + \bar{\lambda}^B, \quad (130)$$

$$[1 - p^S (1 - p^D)] \bar{\lambda}_{k|k-1}^\infty = \bar{\lambda}^B. \quad (131)$$

This equation can be solved if $[1 - p^S (1 - p^D)] \neq 0$, which is ensured if $p^S \neq 1$ or $p^D \neq 0$. As $\mu > 0$, it is met that $p^S < 1$, see (13), so (131) always has a solution. The solution of this equation proves (71). It should be noted that if we had that $p^S = 1$ and $p^D = 0$, there is no steady state solution as $\bar{\lambda}_{k|k-1}$ increases with time.

B. Proof of (72)

Using (69) and (70) and the conditions in Lemma 7, the updated mean number of undetected targets is

$$\bar{\lambda}_{k|k} = (1 - p^D) \left(p^S \bar{\lambda}_{k-1|k-1} + \bar{\lambda}^B \right). \quad (132)$$

In the steady-state solution, $\bar{\lambda}_{k|k} = \bar{\lambda}_{k-1|k-1} = \bar{\lambda}_{k|k}^\infty$, which yields

$$\bar{\lambda}_{k|k}^\infty = (1 - p^D) \left(p^S \bar{\lambda}_{k|k}^\infty + \bar{\lambda}^B \right). \quad (133)$$

Solving this equation, which is possible with $p^S \neq 1$ or $p^D \neq 0$, proves (72).

APPENDIX E

In this appendix, we prove Proposition 8. We first compute the mean and then the covariance matrix.

A. Mean at the time of birth

Using (78) and (24), the mean at the time of birth is

$$\begin{aligned} \bar{x}_{b,k} &= E[E[x_k | t]] \\ &= \frac{\mu}{1 - e^{-\mu \Delta t_k}} \int_0^{\Delta t_k} m(t) e^{-\mu t} dt. \end{aligned} \quad (134)$$

It is direct to check that

$$\bar{x}_{b,k} = \frac{\mu}{1 - e^{-\mu \Delta t_k}} \bar{x}(\Delta t_k)$$

where $\bar{x}(\Delta t_k)$ is the solution of the ODE

$$\frac{d\bar{x}}{dt} = m e^{-\mu t}$$

with initial condition $\bar{x}(0) = 0$ at time $t = \Delta t_k$.

B. Covariance at the time of birth

Following (24), the covariance matrix at the time of birth can be written as

$$P_{b,k} = P_{b,k}^1 - \bar{x}_{b,k} \bar{x}_{b,k}^T \quad (135)$$

where

$$\begin{aligned} P_{b,k}^1 &= E \left[C[x_k | t] + E[x_k | t] E[x_k | t]^T \right] \\ &= \frac{\mu}{1 - e^{-\mu \Delta t_k}} \int [P(t) + m(t) m^T(t)] e^{-\mu t} dt. \end{aligned} \quad (136)$$

It is direct to check that this integral can be computed as

$$P_{b,k}^1 = \frac{\mu}{1 - e^{-\mu \Delta t_k}} \Sigma(\Delta t_k) \quad (137)$$

where $\Sigma(\Delta t_k)$ is the solution of the ODE

$$\frac{d\Sigma}{dt} = [P + m m^T] e^{-\mu t} \quad (138)$$

with initial condition $\Sigma(0) = 0$ from $t = 0$ to $t = \Delta t_k$. Then, to calculate $\bar{x}(\Delta t_k)$ and $\Sigma(\Delta t_k)$, we must simultaneously solve the ODEs in Proposition 8, which also account for the evolution of $m(t)$ and $P(t)$ with time.